PLOS ONE

RESEARCH ARTICLE

The effect of prior long-term recellularization with keratocytes of decellularized porcine corneas implanted in a rabbit anterior lamellar keratoplasty model

Julia Fernández-Pérez[1,2☯], **Peter W. Madden**[1,2☯], **Robert Thomas Brady**[3], **Peter F. Nowlan**[4], **Mark Ahearne**[1,2*]

1 Department of Mechanical, Manufacturing and Biomedical Engineering, School of Engineering, Trinity College Dublin, University of Dublin, Dublin, Ireland, **2** Trinity Centre for Biomedical Engineering, Trinity Biomedical Science Institute, Trinity College Dublin, University of Dublin, Dublin, Ireland, **3** Department of Ophthalmology, Mater Misericordiae University Hospital, Dublin, Ireland, **4** School of Natural Sciences, Trinity College Dublin, University of Dublin, Dublin, Ireland

☯ These authors contributed equally to this work.
* ahearnm@tcd.ie

Citation: Fernández-Pérez J, Madden PW, Brady RT, Nowlan PF, Ahearne M (2021) The effect of prior long-term recellularization with keratocytes of decellularized porcine corneas implanted in a rabbit anterior lamellar keratoplasty model. PLoS ONE 16(6): e0245406. https://doi.org/10.1371/journal.pone.0245406

Editor: Alexander V. Ljubimov, Cedars-Sinai Medical Center, UNITED STATES

Received: December 23, 2020

Accepted: May 19, 2021

Published: June 1, 2021

Data Availability Statement: All relevant data are within the manuscript file.

Funding: MA received funding from European Research Council, grant number 637460 (https://erc.europa.eu/) and Science Foundation Ireland, grant number 15/ERC/3269 (https://www.sfi.ie/). The funders had no role in study design, data collection and analysis, decision to publish, or preparation of the manuscript.

Abstract

Decellularized porcine corneal scaffolds are a potential alternative to human cornea for keratoplasty. Although clinical trials have reported promising results, there can be corneal haze or scar tissue. Here, we examined if recellularizing the scaffolds with human keratocytes would result in a better outcome. Scaffolds were prepared that retained little DNA (14.89 ± 5.56 ng/mg) and demonstrated a lack of cytotoxicity by *in vitro*. The scaffolds were recellularized using human corneal stromal cells and cultured for between 14 in serum-supplemented media followed by a further 14 days in either serum free or serum-supplemented media. All groups showed full-depth cell penetration after 14 days. When serum was present, staining for ALDH3A1 remained weak but after serum-free culture, staining was brighter and the keratocytes adopted a native dendritic morphology with an increase ($p < 0.05$) of keratocan, decorin, lumican and CD34 gene expression. A rabbit anterior lamellar keratoplasty model was used to compare implanting a 250 μm thick decellularized lenticule against one that had been recellularized with human stromal cells after serum-free culture. In both groups, host rabbit epithelium covered the implants, but transparency was not restored after 3 months. Post-mortem histology showed under the epithelium, a less-compact collagen layer, which appeared to be a regenerating zone with some α-SMA staining, indicating fibrotic cells. In the posterior scaffold, ALDH1A1 staining was present in all the acellular scaffold, but in only one of the recellularized lenticules. Since there was little difference between acellular and cell-seeded scaffolds in our *in vivo* study, future scaffold development should use acellular controls to determine if cells are necessary.

Competing interests: The authors have declared that no competing interests exist.

1. Introduction

The limited supply of human corneas for transplantation requires investigation of an alternative supply and one promising solution has been the use of decellularized corneas [1–4]. These corneas may be obtained from human donors whose corneas would otherwise be unsuitable for transplantation [5], but an animal source such as the pig offers a much greater supply of tissue. Decellularized porcine corneal stroma provides a collagen-proteoglycan scaffold with appropriate composition and architecture that inherently supports corneal transparency and cellular repopulation. These corneas have already undergone clinical trials with encouraging results [1–5]. The laboratory work that preceded these trials included implantation of both human or porcine decellularized corneal stroma, primarily using a rabbit model of both interlamellar pocket and anterior keratoplasty [6–11]. These studies indicated that although neovascularization and immune reaction was slight, corneal haze did hamper vision for some time, although corneal transparency eventually began to return as the study length increased [3]. These findings support the concept that decellularized corneal scaffold serves as a template for remodelling [6], but there is always a delay in transparency, or the risk of permanent haze from scar tissue. Although the epithelium rapidly returned to the anterior surface of the scaffold, few keratocytes repopulated the stroma, even after 12 months [7–9, 12]. Such a long delay appears undesirable, as one role of keratocytes is to remodel the stromal extracellular material (ECM) and thereby regulate collagen fibril spacing to restore corneal transparency [13]. However, it has been recognised that even disordered collagen fibrils in ECM can still be transparent [14] if they are not too thick, which is the case with porcine derived scaffold.

Clinically, if the cornea is damaged leaving the ECM intact, quiescent corneal keratocytes proliferate without phenotype switching or scar formation [15]. Maintaining appropriate keratocyte phenotype is vital to preventing them becoming fibrotic, resulting in permanent scar tissue formation [16, 17]. The presence of keratocytes also benefits in nerve re-innervation via neuro-regulatory factor secretion [18]. For these reasons, a limited number of studies have been undertaken to assess the effect of recellularizing the decellularized stroma prior to implantation [10]. In one rabbit host study [10], the porcine scaffold that had been recellularized by injection of human stromal cells and 3 days of culture recovered transparency faster and achieved a more native-like ultrastructure than a decellularized counterpart. In a 12 month long-term study in dogs, decellularized porcine corneas that had been recellularized with human epithelial and stromal cells for 8 days showed improved re-innervation, epithelial integrity and a more normal central corneal thickness, compared with cell-free scaffolds [19].

In acellular clinical studies, where decellularized porcine scaffolds were implanted into the human eye to repair damage from a localised infection, there was a beneficial outcome, without rejection, but with only gradual recovery of transparency and some improvement of visual acuity [1, 3, 4]. The repopulation of the scaffold with keratocytes was slow, as was the healing response compared with using a healthy donated human cornea [1]. In further studies aimed at overcoming such disadvantages, stroma repopulation has been investigated; thin sections of human decellularized scaffold were implanted into patients with advanced keratoconus, but no clear advantage was found between the use of acellular implants compared with those pre-seeded for the short-term of 1 day with autologous adipose mesenchymal stromal cells [5].

Overall, the clinical studies confirm the value of using porcine corneal scaffold, but the potential benefit of re-seeding keratocytes prior to implantation is not clearly established. The first aim of the current study was therefore to examine the *in vitro* recellularization of a decellularized porcine corneal scaffold with human keratocytes over an extended culture period of 28 days and analyse the normality of the resultant cell phenotype. The premise was that, normality established prior to implantation would best result in post-implant transparent tissue.

Human keratocytes were chosen for this investigation as these cells have already shown utility with this model of decellularized porcine scaffolds in the rabbit and offer the most potential for clinical translation [10]. The immunological and healing response in the living host can have a profound effect and there is a need to understand if a native phenotype *in vitro* leads to a transparent cornea after implantation. The second aim was therefore to test if a high cell density recellularized scaffold is superior to a decellularized scaffold using an anterior lamellar keratoplasty (ALK) model in the rabbit.

2. Materials and methods

Isolation and decellularization of porcine corneal lenticules

Porcine eyes were collected a few hours after animal death from an abattoir (Rosderra Meats, Edenderry). The eyes were transported while refrigerated and processed within 12 hours. To process the eyes, they were first trimmed and then decontaminated in 2% iodine solution (Videne, Ecolab, Belgium) in sterile phosphate buffer saline (PBS) for 1 minute with gentle agitation and then washed twice in PBS. The lenticule produced had a smooth, dull, convex, apical surface.

Decellularization was performed as previously described [20] using chemicals purchased from Sigma-Aldrich (Arklow). Corneal lenticules were immersed in decellularization solution containing 0.5% (w/v) sodium dodecyl sulphate (SDS) and 1% (v/v) Triton X-100 in deionised water. To promote removal of cells and denatured proteins, samples were placed in an orbital shaker for 72 hours at ambient temperature, changing the solution every 24 hours. The lenticules were then treated with 10 U/mL of both RNAse and DNAse (Sigma) in 10 mM $MgCl_2$ solution for 1 hour at 37˚C and tube-rotated at 15 RPM. Next, they were washed and rotated with 200 U/mL penicillin and 200 μg/mL streptomycin (Gibco, ThermoFisher, Dublin) in PBS for another 72 hours, changing the solution daily. They were stored at 4˚C in PBS containing the antibiotics until required and, prior to use, equilibrated in culture medium for 24 hours in a humidified incubator at 37˚C with 5.0% CO_2; the method of incubation used throughout the studies.

Scaffold transparency and light transmittance

Light transmittance across the visible spectrum from 350 to 700 nm wavelength was quantified using a spectrophotometer (BioTek Synergy HTX, ThermoFisher) with the scaffold immersed in ultrapure water. Glycerol has been shown to re-establish the thickness and curvature of a swollen cornea [21]. For this reason, the scaffold transmittance was then assessed after immersion in glycerol for 2 hours. Following glycerol treatment, optical quality was also evaluated, by holding the scaffold in a transparent petri dish and then viewing printed text through the base [22].

Scaffold recellularization

Human corneo-scleral rims remaining after keratoplasty were supplied from the Irish Blood Transfusion Service Eye Bank, Dublin after appropriate consent of the donor or next-of-kin and their use received approval from Trinity School of Medicine Ethics Committee. Stromal keratocytes were isolated by explant culture [23]. This method results in the keratocytes becoming fibroblastic. To ensure the cells were consistent across the experiments, they were expanded from cryopreserved stocks and used at passage 4 or 5. Expansion medium consisted of low-glucose Dulbecco's Modified Eagle's Medium (DMEM) (HyClone, Fisher Scientific,

Dublin) supplemented with 10% foetal bovine serum (FBS), penicillin (100 U/mL) and streptomycin (100 mg/mL) (Gibco).

Several methods are available to recellularize a scaffold [11]. Simple seeding on the surface was chosen as the recellularization method in the present study. Recellularization was carried out in a 12-well tissue culture plate (Cellstar, Greiner, Austria). A polytetrafluoroethylene (PTFE) disk was used to cover the tissue culture surface to prevent cells attaching to the plate. The scaffolds were recellularized by seeding 0.1 $x10^6$ stromal cells in 10–15 μl of expansion medium onto the upper surface of the scaffold and allowing cell attachment for 30 minutes of incubation. Scaffolds were then inverted, and a similar application made to the reverse side. Finally, 0.3 $x10^6$ cells were added in 1 mL of expansion medium and cultured with incubation for 14 days, with a change of media every second day.

In the normal cornea, keratocytes are in general quiescent, that upon injury to the cornea are stimulated into repair phenotypes, but a fibrotic response can lead to scarring and loss of corneal clarity [24]. To investigate the phenotype of stromal cells introduced into the scaffold, three different culture conditions were examined. In the first group (the short-expansion group), culture was for 14 days in the serum-supplemented media already described. In the second group, culture was for 28 days in serum-supplemented medium (the long-expansion group). For the third group, the cell seeded scaffolds were cultured for 14 days in the serum-supplemented media and then switched for a further 14 days, (the keratocytic-expansion group), to a serum-free keratocyte medium composed of DMEM/F12 medium (HyClone, ThermoFisher) supplemented with 50 μg/mL ascorbic acid (Sigma) and 1x insulin-transferrin-sodium selenite (Gibco), giving a final concentration of insulin 10 μg/mL, transferrin 5.5 μg/mL and sodium selenite 6.7 ng/mL. This medium has been shown to stabilise the cells into a more native corneal phenotype [25] involving self-assembly of cell distribution on the scaffold [23]. Scaffolds that were to be implanted decellularized, were treated for the same time and keratocytic-expansion media but without cells.

To quantify cell number, DNA was fluorescently stained using a Quant-iT PicoGreen double strand (ds) DNA kit (Molecular Probes, Biosciences, Dublin). The fluorescence was quantified using a spectrophotometer (BioTek Synergy HTX, ThermoFisher) and used to assess total cell number. Comparison was made against the fluorescence of the initial cells applied to the scaffold.

Limbal epithelial cells were isolated by cutting the remaining human donor limbal tissue into quarters and incubating with 2.5 mg/mL dispase (Life Technologies, ThermoFisher) for 1 hour. The cells were removed by scraping the limbal surface with a scalpel blade, then pooled, and centrifuged at 170 G for 5 min. They were then resuspended in epithelial medium and 15 μl placed directly onto the scaffold to give a density of 10^5 cells/cm^2. The epithelium medium was composed of a 3:1 mixture of DMEM (Hyclone, ThermoFisher) combined with Ham's F12 medium (Gibco) and supplemented with 10% FBS (Gibco), 5 μg/mL human recombinant insulin, 0.4 μg/mL hydrocortisone, 2 pM triiodo-L-thyronine, 10^{-5} M isoprenaline hydrochloride, 5 μg/mL transferrin, 180 μM adenine (all Sigma), 10 ng/mL human epithelial growth factor (Source BioScience, Nottingham, UK) and 2 mM L-glutamine, 100 U/mL penicillin and 100 μg/mL streptomycin (all Gibco).

Histology, immunostaining and imaging

Scaffolds were fixed in 4% paraformaldehyde in PBS for 30 minutes, permeabilized with 2% FBS and 0.5% Triton X-100, then stained with 4',6-diamidino-2-phenylindole (DAPI) and phalloidin-conjugated to tetramethylrhodamine, to visualize cell nuclei and the F-actin cytoskeleton, respectively. Imaging was performed on a laser scanning confocal microscope (SP8,

Leica). Afterwards, the scaffolds were embedded in paraffin wax and 6 μm thick slices were cut using a microtome (RM2125, Leica Microsystems, UK) and mounted on glass slides (Superfrost plus, ThermoFisher). Native porcine corneas and decellularized scaffolds were stained by three methods: Haematoxylin and eosin (H&E), Alcian blue and picrosirius red, to distinguish cells, glycosaminoglycans (GAG) and collagen, respectively.

Where antibody staining followed paraffin wax embedding, antigens were retrieved by heat-mediated citrate buffer. Primary antibodies were: Aldehyde dehydrogenase ALDH1A1 (Ab9883) and ALDH3A1 (Ab76976) from Abcam (Cambridge, UK). Both were used as the ALDH3A1 is a rabbit sourced antibody, making it unsuitable as a primary in the rabbit, and also, unlike humans, rabbits primarily express ALDH1A1 in the cornea, with negligible amounts of ALDH3A1 [26]; alpha smooth muscle actin, α-SMA (Ab7817); fibronectin (Ab6328) from Abcam; collagen Ia (sc-59772) from Santa Cruz Biotechnology (Heidelberg, Germany); collagen III (GTX26310) from GeneTex (Insight Biotechnology, London, UK); and keratocan (HPA039321) from Atlas Antibodies (Cambridge Bioscience, Bar Hill, UK). Appropriate secondary antibody conjugated with AlexaFluor 488 (Abcam) was visualised on a laser scanning confocal microscope (SP8, Leica). Negative controls involved use of the secondary antibody alone. Human corneal tissue was used as a positive control for keratocan and ALH3A1 staining while vascularized limbal tissue was used as a positive control for α-SMA. Cross-reactivity of a nucleolar stain for human cells meant that we were unable to confirm the survival of human cells after the rabbit ALK.

The density of the scaffold limited imaging to less than 100 μm from the surface. To assess the extent of cell position in the deeper layers, for each sample, 3 scaffold cross-sections were cut, and every DAPI-labelled nucleus was classified as a cell in the section. The closest scaffold surface was assumed to be the origin of each cell, and the distance from that surface to the nucleus was measured for each. Cells were grouped into 20 μm depths and counted to quantify the extent of cell penetration.

Biochemical analyses

Samples were held frozen at -80˚C prior to biochemical analysis. All weights were standardised against the dry weight of the sample. For the DNA, glycosaminoglycans and collagen quantification, native lenticules and decellularized scaffolds were freeze-dried then weighed. The freeze-dried samples were then digested in 3.88 U/mL of papain solution and tube-rotated at 60˚C for 18 hours to disrupt the tissue.

DNA content. The DNA was fluorescently stained using a Quant-iT PicoGreen double strand (ds) DNA kit (Molecular Probes, Biosciences, Dublin) and quantified against a control standard by spectrophotometry at 480 nm excitation and 520 nm emission wavelengths. The extent of DNA fragmentation was also measured after extraction of the DNA using a DNeasy kit (Qiagen, ThermoFisher) and separation of the fragments by electrophoresis on a 3% agarose gel.

Glycosaminoglycans content. Determination of GAG used a 1, 9 dimethylmethylene blue dye assay (Blyscan, Biocolor, UK). Briefly, 10 μl of papain digested sample was incubated with the dye for 30 minutes at ambient temperature with tube-rotation, then centrifuged at 15,000 G for 10 minutes and the supernatant removed. The remaining pellet was treated with the dye dissociation reagent and the dye density measured with a spectrophotometer at 656 nm excitation wavelength. Known quantities of GAG were processed in the same way to obtain a dye absorption standard curve.

Collagen content. The collagen content was determined using a hydroxyproline assay [27] which is based upon the fixed ratio of hydroxyproline to collagen of 1 to 7.69 [28]. To

measure the hydroxyproline, a 10 μl of papain digested sample was dissociated with 38% HCl at 110˚C for 18 hours and then dried for 48 hours at 50˚C. Serial dilutions of trans-4-hydroxy-Lproline (Fluka, ThermoFisher) in papain solution were used to obtain a standard range. Samples and standards were incubated for 20 minutes at ambient temperature with n-propanol buffer and chloramine-T to oxidize the hydroxyproline and stained with a 2,4-dimethoxybenzaldehyde dye for 20 minutes at 60˚C. The dye concentration was quantified at 570 nm excitation wavelength using a spectrophotometer.

SDS contamination quantification. Following decellularization, the extent of SDS contamination of the scaffold was measured by a methylene blue assay, whereby the complex of the SDS anion and dye cation is quantified by dye light-absorption. Freeze-dried scaffolds were weighed, vortexed in 1 mL of deionised water and then macerated for six hours. A 250 μl sample was then taken and vortexed with an equal volume of 250 μg/mL methylene blue solution (Sigma-Aldrich), and 1 mL of chloroform added. The mixture was centrifuged on a benchtop centrifuge to separate the aqueous supernatant. The absorbance of the chloroform and dye infranatant was measured at 665nm using a plate reader (BioTek Synergy HTX). Absorbance was quantified against a standard of deionised water and serial dilutions of 0.5% w/v SDS.

Gene expression

Trizol (Invitrogen) was used to extract RNA from cells in the scaffold in combination with homogenisation (IKA T10 basic, Sigma) [29]. Chloroform was then added and vortexed, prior to centrifugation at 4˚C for 15 minutes at 12,000 G to remove debris. To precipitate the RNA, the supernatant was transferred into a new tube and diluted with the same volume of isopropanol and 3 μl of Glycoblue (Life Technologies, ThermoFisher). After overnight freezing to -20˚C, centrifugation was repeated, and the supernatant discarded. The pellet was washed in 70% ethanol in RNAse-free water, centrifuged, the supernatant removed, air-dried, then dissolved in RNAse-free water.

RNA yield and purity were measured using a NanoDrop-1000 (ThermoFisher). A high capacity cDNA reverse transcription kit (Invitrogen) was then used to convert RNA into cDNA. Real-time PCR was performed using TaqMan Universal Master Mix II (ThermoFisher) along with the following TaqMan primers: glyceraldehyde-3- phosphate dehydrogenase (GAPDH, Hs02758991_g1), aldehyde dehydrogenase 3A1 (ALDH3A1, Hs00964880_m1), alpha smooth muscle actin (α-SMA) (ACTA2, Hs00426835_g1), keratocan (KERA, Hs0055 9942_m1), collagen I (COL1A1, Hs00164004_m1), lumican (LUM, Hs00929860_m1), decorin (DCN, Hs00754870_s1) and CD34 (Hs00990732_m1). The genes of interest were normalized against glyceraldehyde 3-phosphate dehydrogenase using the $\Delta\Delta C_t$ method. Calculated values were expressed as a power of $2^{-\Delta\Delta Ct.}$ All values were normalized against the serum-expanded cells growing in tissue culture prior to seeding onto the scaffolds.

Axonal outgrowth test

Dorsal root ganglion (DRG) have been used to validate the ability of nerves to innervate a collagen hydrogel scaffold *in vitro* which was subsequently confirmed in a 12 month animal model [30]. To perform a similar *in vitro* test, DRGs were isolated from adult rats, rinsed in expansion media and placed directly onto scaffold that had been removed from its expansion medium, but left moistened. The ganglia were left for 1 hour of incubation and then 1 mL of DMEM, supplemented with 10% FBS and 10 ng/mL NGF (Sigma), was added to cover it. Media was changed every 3 days. After 14 days in culture, scaffolds were fixed in paraformaldehyde and immunostained with the neural cell marker βIII-tubulin (Sigma).

In vivo scaffold implantation in rabbits

Eight female New Zealand rabbits (21–23 weeks old, 2.75–4.0 kg) were used for the experiment, randomly divided into 2 groups. Additional rabbits were used to establish the model. The selection of decellularized or recellularized samples was randomised and the surgical and histological examination teams were unaware of the implant cellularization status until the data collection was complete. This resulted in 3 acellular and 5 cellular implants. Animal welfare and surgery procedures were approved by Research Ethics Committees of both Trinity College Dublin (301107–1001) and Dublin City University (DCUREC/2018/253) and the project authorised by the Health Products Regulatory Authority (AE19136/PO93). The right eye of each rabbit was used for the anterior lamellar keratoplasty, whilst the left eye was untreated, as a control. One animal group received decellularized porcine scaffold left acellular, and the other group, scaffold that had been recellularized with human stromal cells. Both scaffolds were cultured using the keratocytic-expansion protocol (S1 Fig).

As detailed elsewhere [31], prior to surgery the rabbits were first pre-medicated with subcutaneous buprenorphine (0.03 mg/kg) (Buprecare, Animalcare Group, York, UK) and then anesthetized with intravenous ketamine (10 mg/kg) (Hameln pharmaceuticals Gloucester, UK) and xylazine (3 mg/kg) (Sedaxylan, Dechra, Shrewsbury, UK) whilst oxygen was administered through a face mask to maintain oxygen saturation. To extend anaesthesia, 0–5% gaseous isoflurane (Isoflurin, Vetpharma Animal Health, Barcelona, Spain) was used and additional intravenous ketamine and xylazine given as a bolus, as necessary.

After the epithelium had been debrided with 70% ethanol over the implant site, the recipient cornea was trephined to 250 μm depth using a 6.0 mm diameter Barron radial vacuum trephine (Barron Precision Instruments, Grand Blanc, MI, USA) and the stromal tissue excised by the same method as with the porcine tissue. Scaffolds were orientated, convex side apical, to maintain the native density of the scaffold collagen fibrils. Scaffolds were sutured into the rabbit defect with 16 interrupted 10–0 nylon sutures (Serag Wiessner, Naila, Germany or Ethicon, Medray, Dublin) and the knots buried to reduce irritation. Immediately after surgery the eye was irrigated with the broad-spectrum antibiotic, cefuroxime (Aprok, Biopharma S.R.L., Roma, Italy).

Under the control of a veterinarian, postoperative analgesia of subcutaneous buprenorphine (0.01 mg/kg) was administered twice a day for at least 3 days. Postoperative topical corticosteroid, (Betnesol 0.1% w/v, RPH Pharmaceuticals AB) drops or ointment, and topical antibiotic chloramphenicol drops (Minims chloramphenicol 0.5% w/v, Bausch Health, Dublin) or ointment (1% w/w, Martindale Pharma, UK), were applied up to four times daily.

Post-operative eye examinations were performed at: 1, 3, 7, 14 days and 1, 2 and 3 months. At these times, slit lamp biomicroscopy (Portable slit lamp, Reichert, Buffalo, NY, USA) was used for the general assessment of the health of the anterior segment of the eye and intraocular pressure was monitored by contact tonometry measurement (Tonovet plus, Icare, Vantaa, Finland). The extent of re-epithelialization of the implants was confirmed by fluorescein staining (Minims fluorescein sodium 1%, Bausch Health). At 3 months post-operative, the rabbits were euthanized with an overdose of intravenous sodium pentobarbital (Dolethal, Vetoquinol, Towcester, UK). Eye globes were removed, photographed and examined by optical coherence tomography (OCT) with an OC LabScope (Lumedica, Durham, NC, USA). They were then fixed in 10% formalin for 24 hours at ambient temperature, the cornea was then excised and embedded in paraffin wax for histological and immunohistochemical analysis.

Statistical analysis

All in vitro experiments were performed three times with a minimum of three replicates. Data are presented as the mean ± SD. Statistical analyses were calculated using GraphPad Prism 6

(GraphPad Software, San Diego, USA). An unpaired two-tailed *t*-test was used to compare two groups and a 2-way ANOVA and Tukey post-hoc analysis when comparing three or more groups. Statistical significance was accepted at a level of $p < 0.05$.

3. Results

Decellularization

Decellularization requires cell removal and DNA minimisation without marked removal of other constituents or the addition of chemical contamination. DAPI and H&E staining demonstrated that the cellular structure of native tissue (Fig 1A) was removed by decellularization and no nuclei could be seen (Fig 1B). Supporting this, Picogreen quantification of DNA showed a reduction from the 728.9 ± 110.2 ng/mg of the native cornea to 14.89 ± 5.56 ng/mg following decellularization (Fig 1C). The display of fraction size of DNA > 1500 base pairs, taken to be supercoiled DNA, was a bright band for the native cornea, while only faint smearing for the decellularized scaffold lanes (Fig 1F). GAGs were also reduced, visualised by the reduction of Alcian blue staining (Fig 1A and 1B) and quantified by the biochemical assay (Fig 1D); in the native cornea GAG was 40.13 ± 2.15 μg/mg, while in the decellularized this was 10.22 ± 5.44 μg/mg.

Collagen was not noticeably reduced by decellularization, as seen by picrosirius red staining (Fig 1A and 1B) and quantified by the hydroxyproline assay (Fig 1E). The collagen content rose from 0.59 ± 0.07 mg/mg to 0.63 ± 0.07 mg/mg following decellularization, as its proportion increased as other constituents were reduced. From the histological images, the collagen structure appeared similar between the groups, other than the collagen in the anterior third of the decellularized scaffold appeared more separated, as if there had been more osmotic swelling resulting in lacunae.

To assess chemical contamination of the scaffold, the concentration of SDS after decellularization was measured to be 52 ± 23 μM.

In PBS the scaffold showed haze, but when dehydrated in glycerol there was good optical clarity (Fig 2). Light transmittance was poor in water (0.95% at 300 and 43.72% at 700 nm), but when transferred to glycerol it improved comparable with that of the native tissue.

In vitro stromal repopulation

Keratocytes were able to penetrate into the scaffolds regardless of the culture conditions examined (Fig 3A). Confocal microscopy of the recellularized scaffold demonstrated a higher cell density close to the surfaces, diminishing as the depth increased (Fig 3B). The count of cells for every 20 μm of depth in corneal sections confirmed density decreased with depth (Fig 3C) and all three culture conditions had a similar depth/density profile. The median depth was 66 μm for the short-expansion and 71 μm for both the long-expansion and the keratocytic-expansion. Measurement of keratocyte cell count by total DNA quantity in the scaffold did not vary significantly between the three culture conditions (Fig 3D). Deeper cells had a more native organisation with a dendritic morphology and interconnecting pseudopodia that appeared to form a 3D network.

The gene expression of cells in the repopulated scaffolds was assessed by quantitative PCR (Fig 4). Keratocyte markers for the crystallin ALDH3A1, CD34 and small leucine-rich extracellular matrix proteoglycans keratocan, decorin and lumican, as well as collagen I and the fibrotic marker α-SMA were all significantly up-regulated with the keratocytic-expansion treatment compared with the short- and long-expansions.

Cell phenotype was further analysed via immunohistochemistry for ALDH3A1, keratocan and α-SMA (Fig 5) in the scaffold. Native human central cornea and limbus were used as controls. The short-expansion group was negative for all three markers. The long-expansion group and keratocytic-expansion were also negative for keratocan and α-SMA. However, the

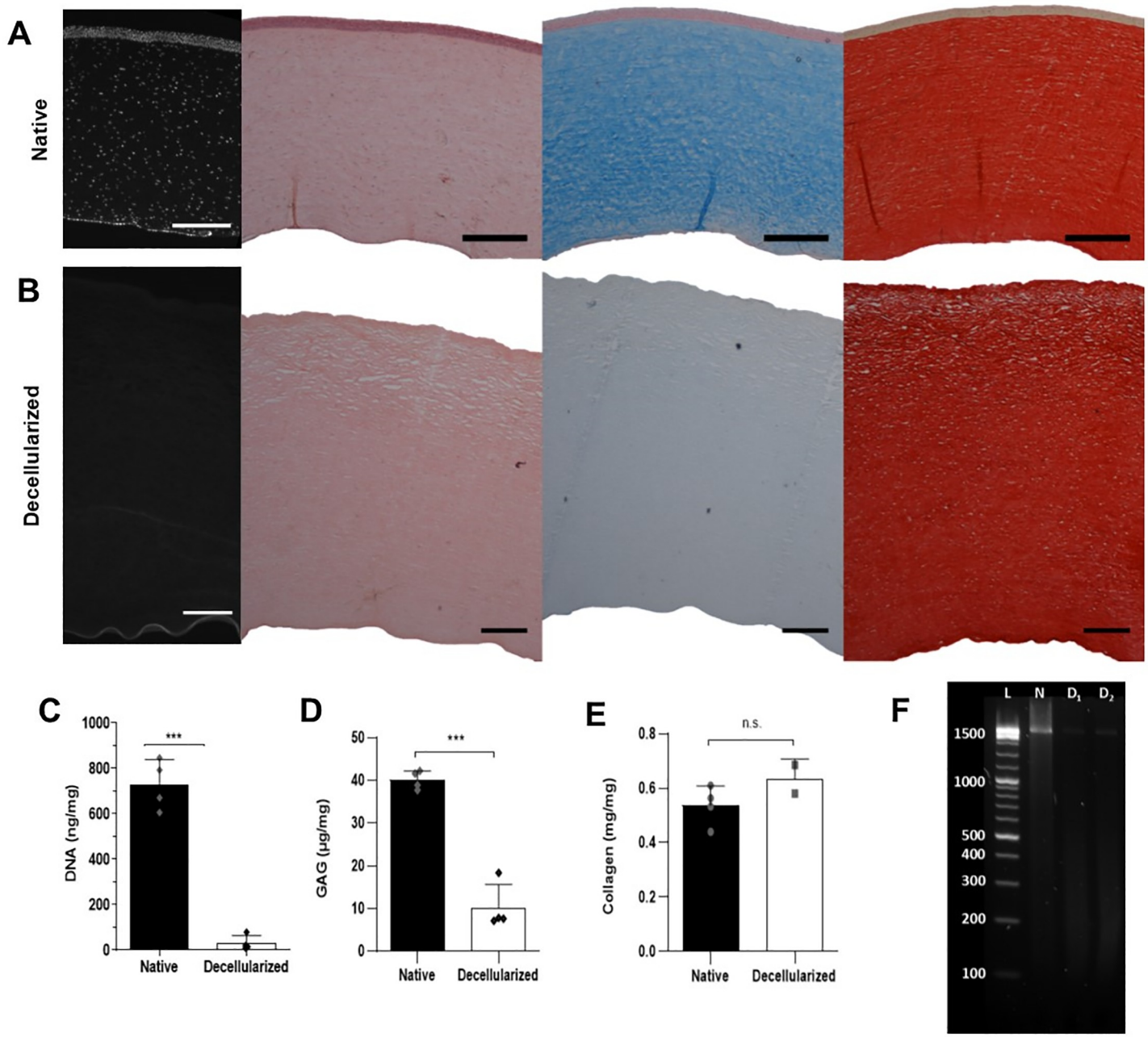

Fig 1. Evaluation of porcine cornea decellularization. A) Native cornea and B) decellularized scaffold, from left to right stained with, DAPI, H&E, Alcian blue or picrosirius red. Black scale bar = 500 μm, white = 250 μm. Quantification of native cornea and decellularized scaffold C) DNA, D) glycosaminoglycans and E) Collagen. $p^{*} < 0.05$, $p^{**} < 0.01$, $p^{***} < 0.001$. F) Agarose gel electrophoresis of DNA from native cornea (N) and decellularized scaffold (D1 and D2). Ladder (L).

https://doi.org/10.1371/journal.pone.0245406.g001

long-expansion showed faint ALDH3A1 staining and the keratocytic-expansion had much brighter expression indicating greater maturity.

In vitro epithelial growth confirmation

Freshly isolated human limbal epithelial cells colonized the surface when seeded onto the scaffold. There was confirmation of native morphology, as the cells adopted the typical cobblestone appearance with a high nucleus-to-cell size ratio (Fig 6A).

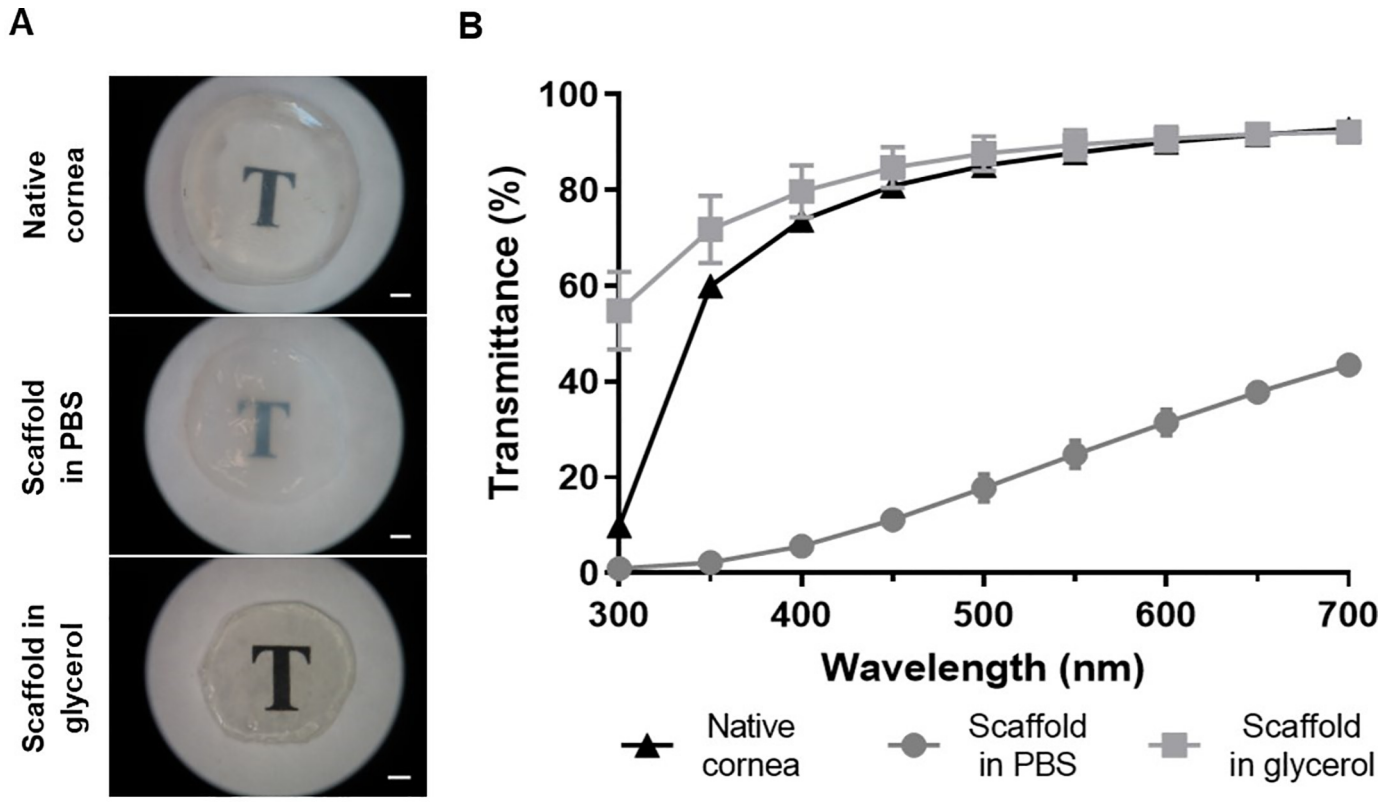

Fig 2. Scaffold optical clarity and light transmission. A) Macroscopic optical clarity. Scale bar = 1 mm. B) Light transmittance spectra.

https://doi.org/10.1371/journal.pone.0245406.g002

In vitro axonal growth confirmation

Axon regrowth into the scaffold for 14 days was demonstrated by βIII-tubulin-positive neurites from the rat DRG extending through to the centre of the scaffold (Fig 6B).

In vivo implantation of scaffolds

***In vivo* operative procedure.** The scaffolds were successfully implanted using conventional surgical technique (Fig 7A and 7B). Some scaffolds appeared contracted prior to surgery, but readily relaxed into place. Implants were easily transferred and positioned with conventional surgical instruments whilst displaying excellent suture retention strength characteristics. OCT showed that the defect was repaired with close apposition of the scaffold with the native tissue (Fig 8B).

***In vivo* post-operative progress.** Fluorescein staining demonstrated regeneration of the epithelium over most of the scaffold surface 3 weeks post-implantation (Fig 9A and 9B). By 2 months there was complete cover (Fig 9C and 9D). Over the experimentation period, the scaffolds appeared to decrease in diameter. The sutures became looser, to the point that a few were unburied and were removed for animal welfare. Although the original whiteness of the scaffold did subside, with some areas appearing to be more translucent. Neovascularization developed, but intraocular pressure did not elevate.

Three months after implantation, decellularized and recellularized showed comparable epithelial layer re-establishment. Transparency had not returned to the implanted scaffolds (Fig 7C and 7D). The location of the opacification appeared to be in the anterior layer.

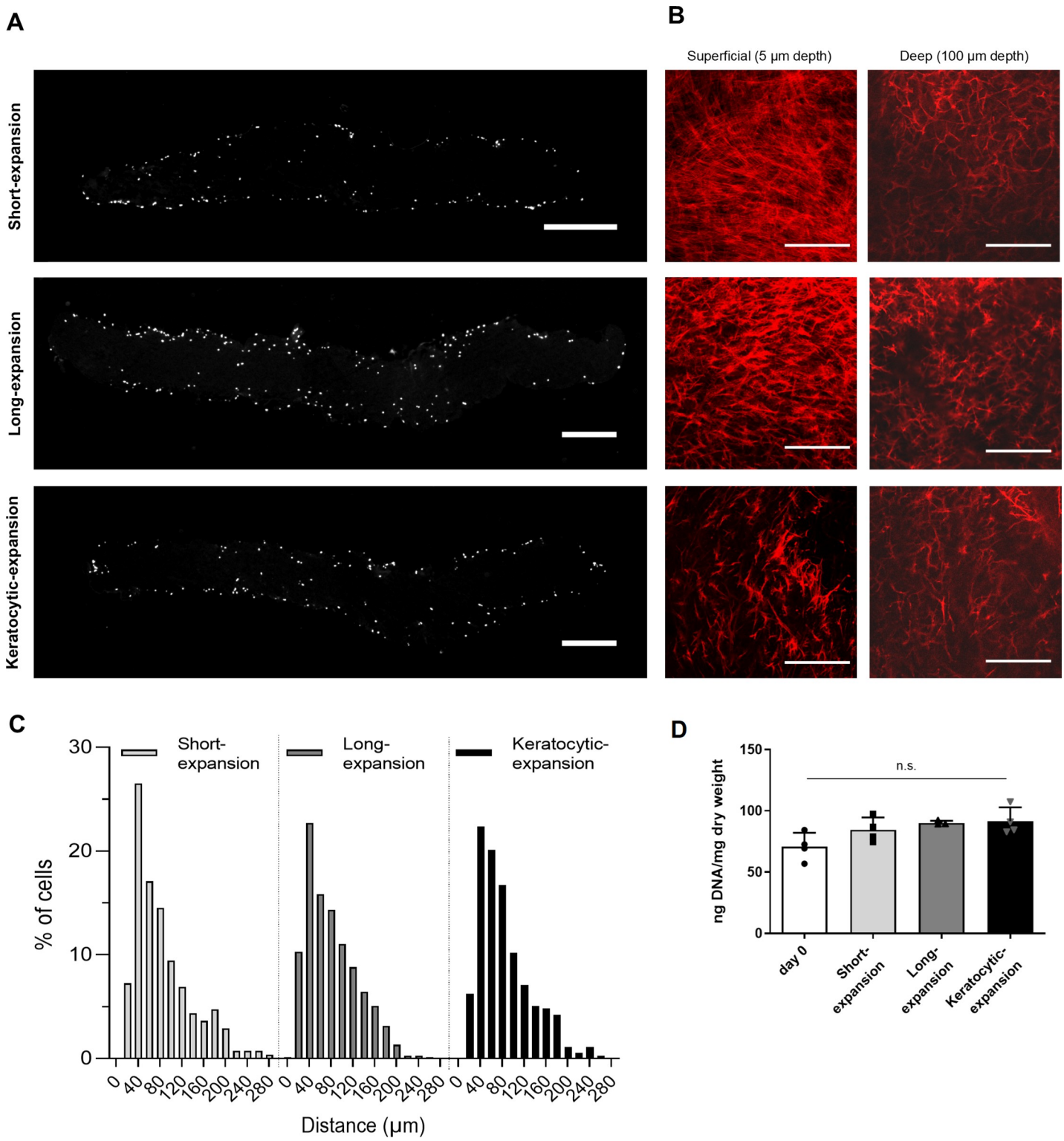

Fig 3. Analysis of the effectiveness of recellularizing scaffold with human keratocytes. A) Longitudinal sections of recellularized scaffolds of keratocytes stained with DAPI nuclear staining following 14 or 28 days of serum culture (short and long expansion), or 14 days of serum culture then 14 days without serum (keratocytic expansion). Scale bar = 500 μm. B) Actin staining of keratocytes at a superficial depth (5 μm), and deep depth (100 μm). Scale bar = 200 μm. C) Quantification of number of keratocytes grouped by distance migrated from the surface of the scaffold. D) Cell quantification of recellularized scaffolds by total DNA (n.s. = not significant).

https://doi.org/10.1371/journal.pone.0245406.g003

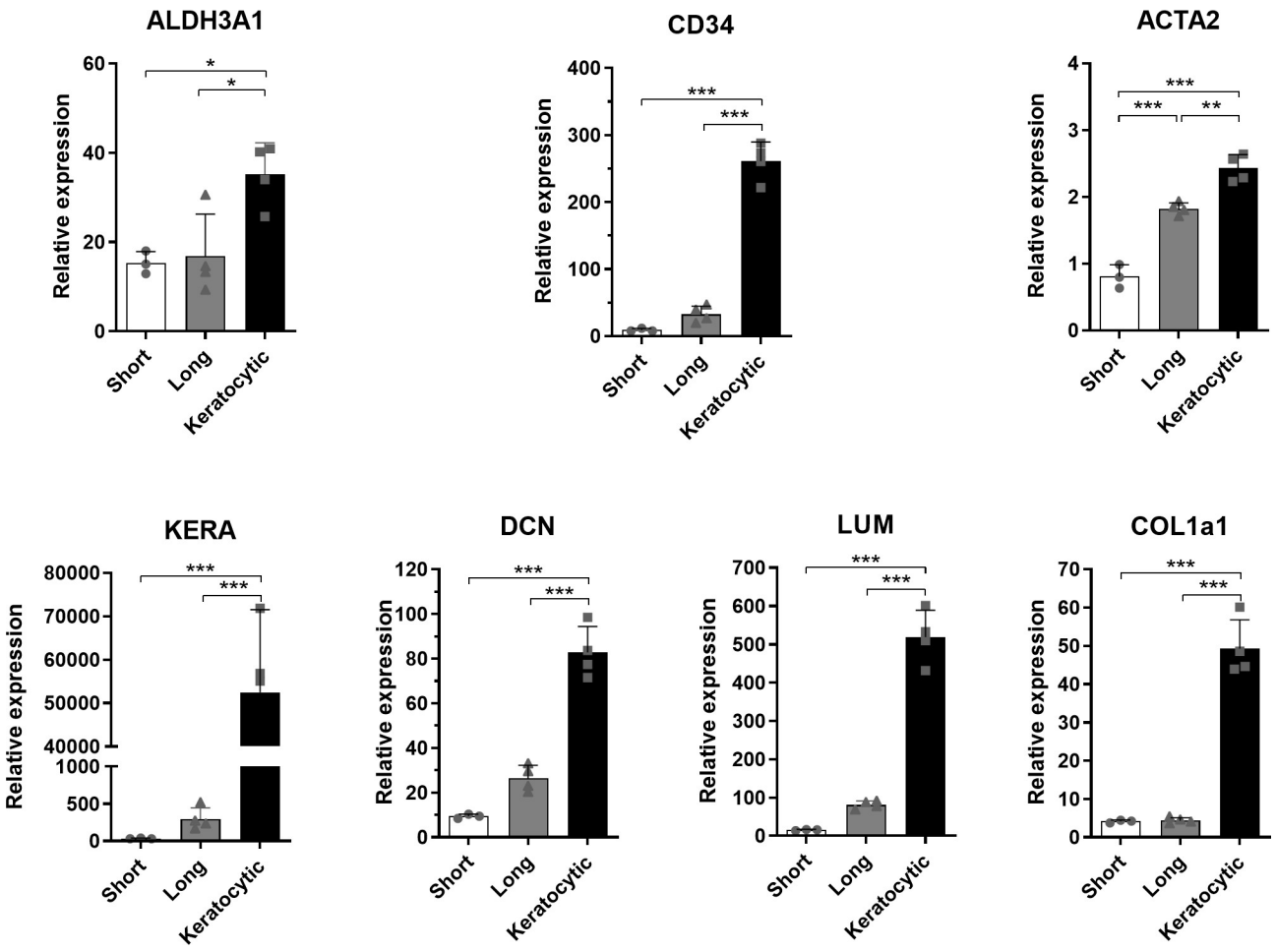

Fig 4. Gene expression analysis of keratocytes in the scaffold. There is a significant difference for all gene expression compared with that of the keratocytic-expansion. (n = 3–4). * $p < 0.05$, ** $p < 0.01$, *** $p < 0.001$.

https://doi.org/10.1371/journal.pone.0245406.g004

Examination of post-mortem eyes

The animals were euthanized, and OCT showed that the scaffold remained in place, but it appeared swollen (Fig 8C). Three regions were discerned: a posterior native tissue, a central scaffold and an anterior area. The eyes were removed, and the corneas used for histological analysis, with the unoperated eye as control.

***Post-mortem* corneal ECM appearance.** The stroma of both groups gave the appearance of three layers: a posterior native area, a central scaffold area and an anterior regenerating area (Figs 10 and 11). The central scaffold area appeared denser than the other two areas when viewed with picrosirius red staining. The scaffold area was strongly positive for collagen I, indicating retention of the implanted collagen in both groups. Collagen III was localised to the apical area and adjacent to the scaffold in the posterior native area; it was not present in the scaffold itself. Similarly, fibronectin was also located in this apical area, particularly with the recellularized group (Fig 10). Generally, the two groups were similar other than in the recellularized tissue the anterior regeneration area appeared denser and the fibronectin more pronounced.

***Post-mortem* corneal cell appearance.** H&E staining showed that there was a complete epithelial covering of all samples. This was at least 2 to 3 cells deep (Fig 11A). There was a sparse, apparently normal, distribution of cells in the central scaffold and posterior native area

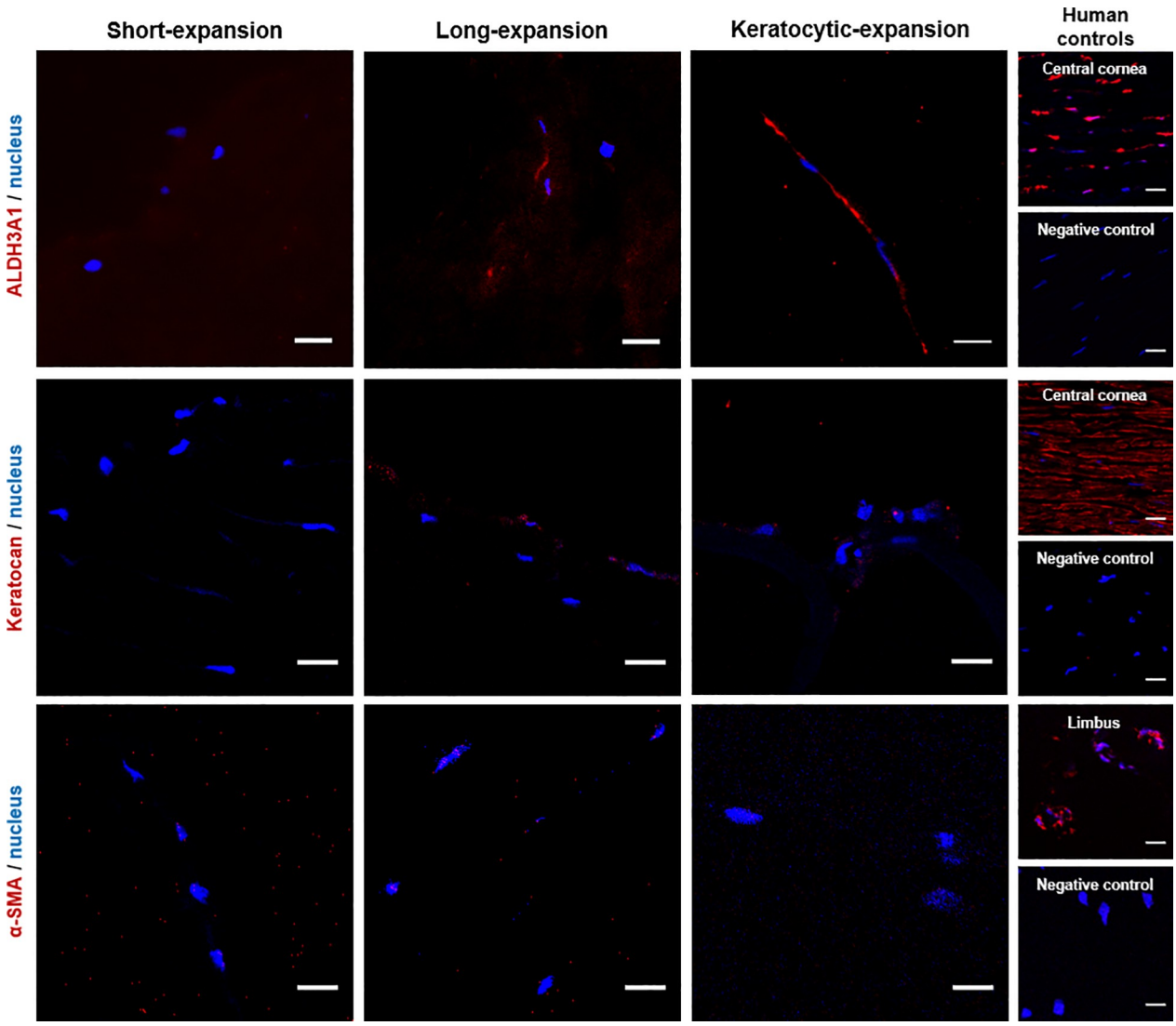

Fig 5. Phenotype of keratocytes in the scaffold. Keratocyte markers, ALDH3A1 and keratocan. Fibrotic marker α-SMA. Nucleus, DAPI nuclear staining (Scale bar = 20 μm).

https://doi.org/10.1371/journal.pone.0245406.g005

of both groups (Fig 11A and 11B). The anterior area appeared to be regenerating, with an increased density of cells. The corneal endothelium was intact in all cases.

There was positive cell staining for ALDH1A1 in the epithelium, the native stroma and endothelium (Fig 11B). ALDH1A1 positive cells were also sparsely distributed in the central scaffold area of all of the decellularized and one of the recellularized implants. With α-SMA staining (Fig 11C), there was extensive staining in both groups in the anterior regenerating area, indicating fibrotic cells. Stained cells were also present at blood vessels.

4. Discussion

Decellularization effectiveness

There are many decellularization methods that use physical, chemical, or enzymatic methods, often in combination [11]. Decellularization is always a balance; it has to be sufficiently

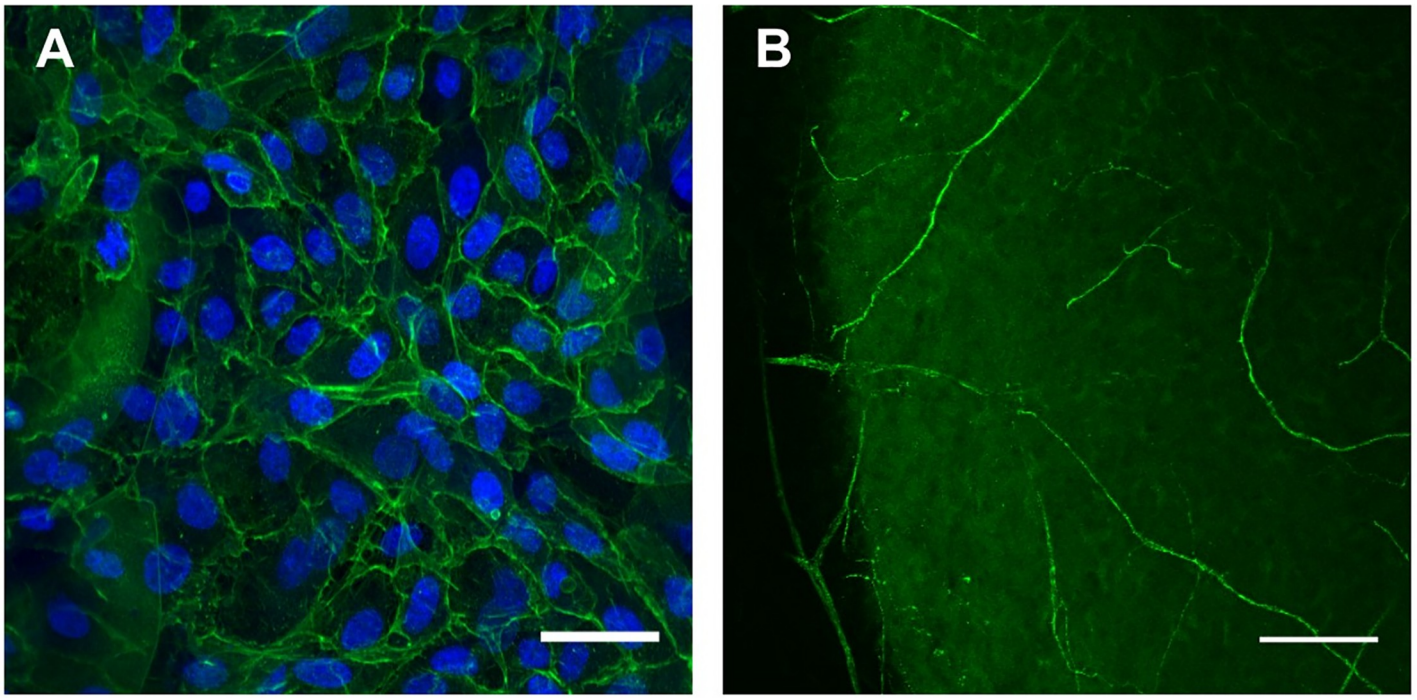

Fig 6. Confirmation of *in vitro* recellularization of porcine scaffold. A) Human corneal epithelial cells on the scaffold surface (blue = nuclei stained with DAPI, green = F-actin). Scale bar = 50 μm. B) Rat DRG βIII-tubulin-positive neurites permeate the scaffold. (Scale bar = 100 μm).

https://doi.org/10.1371/journal.pone.0245406.g006

aggressive to remove those cellular components that can cause immunogenic problems following implantation, whilst at the same time being gentle enough to retain the natural environment of the cornea to ensure normal cellularization and function.

Previous studies with the cornea have proposed that a decellularization treatment of NaCl plus a nuclease has advantages over the use of SDS alone. The NaCl method kept the epithelial basement membrane intact and supported the growth of epithelial cells, whereas SDS could not [32]. Also SDS caused high levels of fibril disorganization and poor optical behaviour of these corneas [33]. SDS is effective at decellularization, particularly to remove cell nuclei, but it can be cytotoxic if retained [34]. Combining multiple detergents allows for more complete detergent removal [35] and decreased adverse immune response *in vivo*, but it does increase ECM loss [36], as with the cornea [9, 37]. To promote removal of SDS, Triton-X100 has been used as a second decellularizing agent [35]. In the present study, we used these dual detergents along with dual nucleases to successfully remove over 95% of dsDNA. This achieved levels below the minimal criteria of <50 ng dsDNA mg dry weight, <200 bp DNA fragment length and lack of visible nuclear material in tissue sections stained with DAPI or H&E, that has previously been shown in multiple studies to allow constructive tissue remodelling whilst avoiding adverse cell and host responses [38, 39]. In our study, the decellularization did reduce the GAGs to less than one quarter of that of the native cornea, but the collagen appeared intact. Although SDS does disrupt the basement membrane of human corneas [32], we showed that epithelial cells were able to repopulate the anterior scaffold surface, both *in vitro* and *in vivo*, and our dual decellularization agents and dual nucleases give certainty of adequate cellular immunogens removal. The scaffold also demonstrated adequate optical behaviour with glycerol preparation.

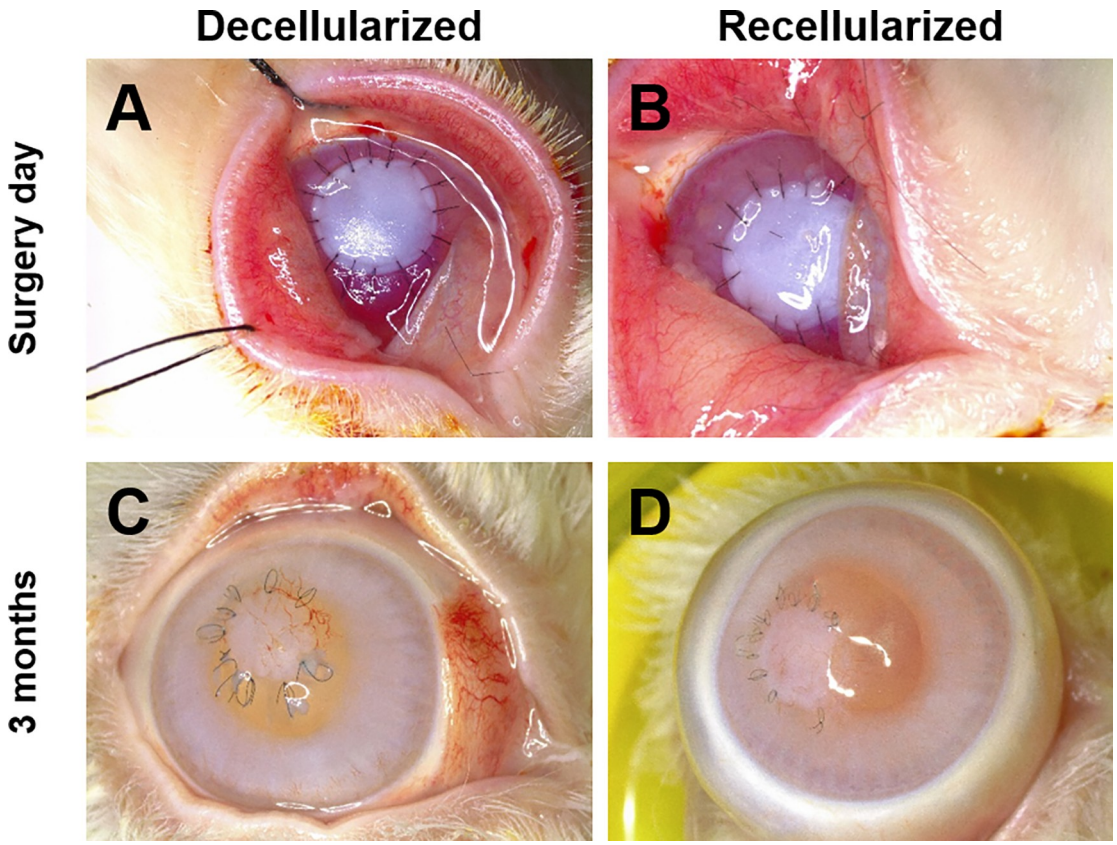

Fig 7. Macroscopic appearance of scaffold in the rabbit eye. Decellularized scaffold (left) with a recellularized scaffold (right). A & B) Day 0. C & D) 3 months post-implantation. At implantation the scaffold was an opaque white. At 3 months both the decellularized and recellularized implants showed some translucent areas, but overall transparency was not recovered and neovascularization had developed.

https://doi.org/10.1371/journal.pone.0245406.g007

The human cornea accepts allogenic tissue more readily than other tissues, with normal corneal avascularity conferring some immune privilege, such that HLA matching is not usually required if combined with topical immunosuppression. However, humans have pre-formed antibodies to some epitopes, and these can result in the rejection of xenotransplants. For example, native porcine tissue contains galactose-alpha- 1,3-galactose (α-Gal) [40] and also N-glycolylneuraminic acid (NeuGc), a non-Gal red blood antigen. These xenoantigens can trigger rejection in pig-to-human implants. In the current study we did not quantify such epitopes, but note that the expression of both Gal and NeuGc have previously been shown to be greatly reduced after decellularization [41]. Additionally, genetically-engineered pigs which express reduced xenoantigens could be used for tissue supply to reduce the human immune response [42].

The detergents used for decellularization can also invoke an immunological problem in their own right. With muscle tissue [43], inadequate extraction of SDS following decellularization resulted in a foreign body response *in vivo*, whereas with a more rigorous extraction the scaffold integrated into the defect with lower levels of inflammatory and fibrosis-related gene expression. In the present corneal study, the scaffold washing method was more intense and of longer duration than the method demonstrated as effective with the muscle, giving in the cornea the same magnitude for the low residual SDS concentration, even before the 28 days of recellularization.

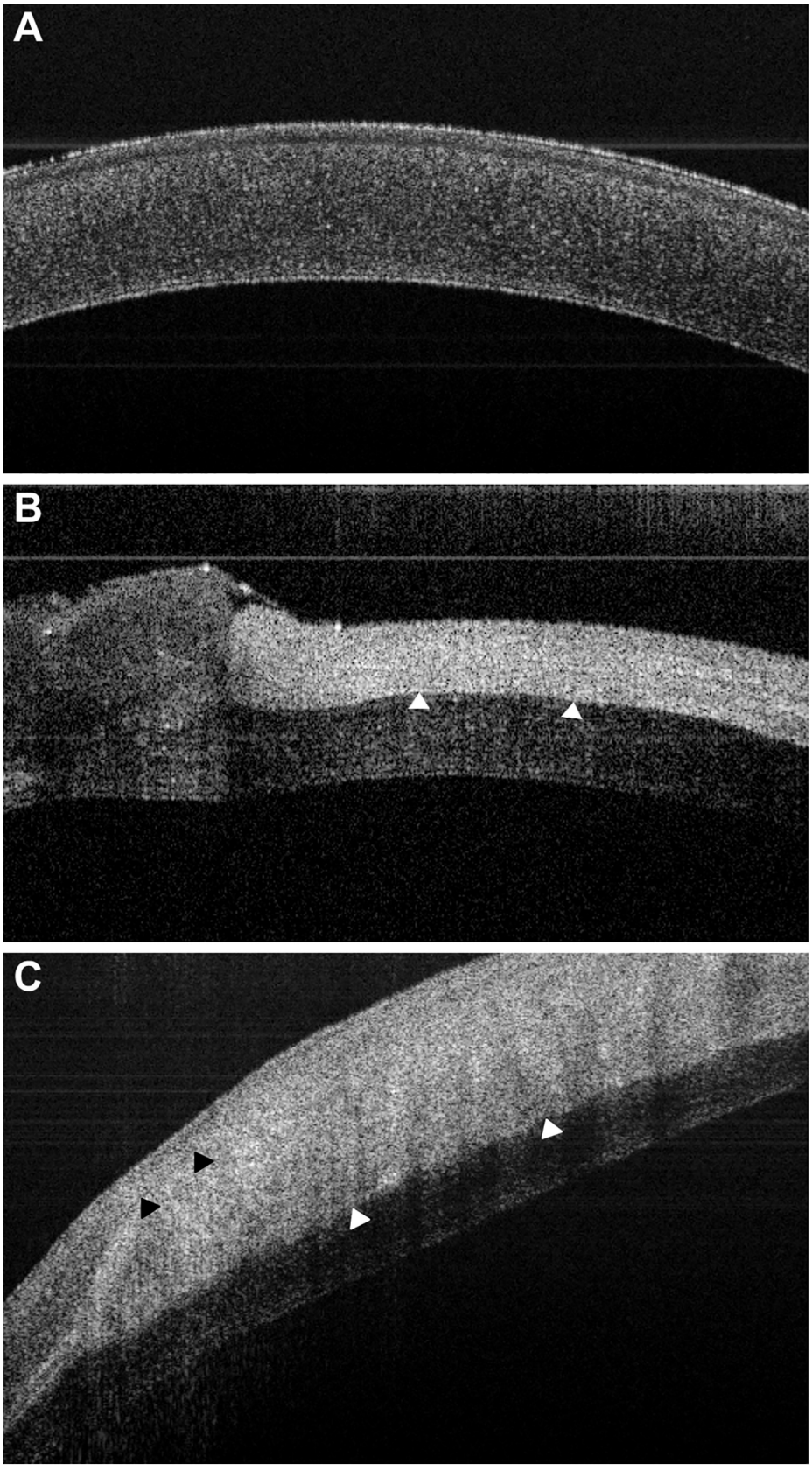
A
B
C

Fig 8. OCT of the rabbit eye. A) Normal un-operated cornea. B) At the time of surgery, day 0. C) 3 months post-surgery. At day 0 the scaffold can be seen to be well-apposed with native tissue (white arrows) repairing a deep defect. At 3 months post-surgery an apparent regeneration area can also be seen anterior to the scaffold (black arrows).

https://doi.org/10.1371/journal.pone.0245406.g008

Stromal recellularization

Human keratocytes were used as the cell source for stromal repopulation. The lack of a significant difference between the DNA quantities and the cell depth/density profiles of the three expansion groups appears to indicate that the cell population had reached its peak density within the first 14 days of culture, the short-expansion. Thus, the additional 14 days in the long-expansion or keratocytic-expansion conditions may not be needed to improve cell density, but the extra time may ensure the appropriate phenotype is achieved. There are several possible reasons for no significant increase in cell number being detected over the culture period. The most likely explanation is that not all cells remained attached to the scaffold, particularly after initial seeding. In addition, it is likely the cells subsequently underwent migration rather than proliferation when seeded onto the scaffold. It is also possible that the division of cells broadly matched cell death.

Although after 3 weeks, even with serum [33], keratocytes have been shown to express high levels of ALDH1 protein (a marker of mature keratocytes), unfortunately serum also activates

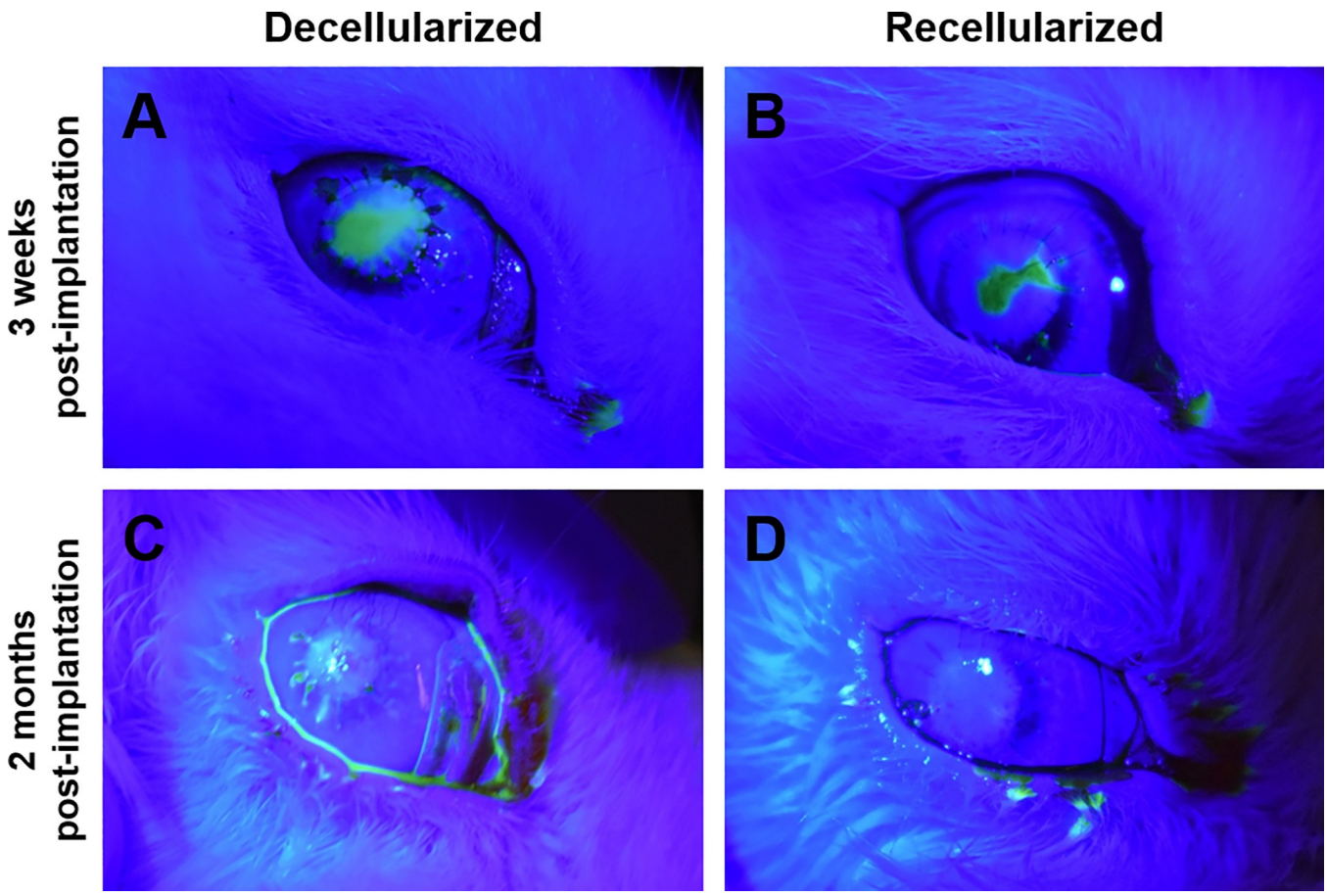

Fig 9. Fluorescein staining of the rabbit eye. A, C) 3 weeks and B, D) two months post-implantation. With both groups the epithelial barrier is not complete at the earlier time, but is intact later.

https://doi.org/10.1371/journal.pone.0245406.g009

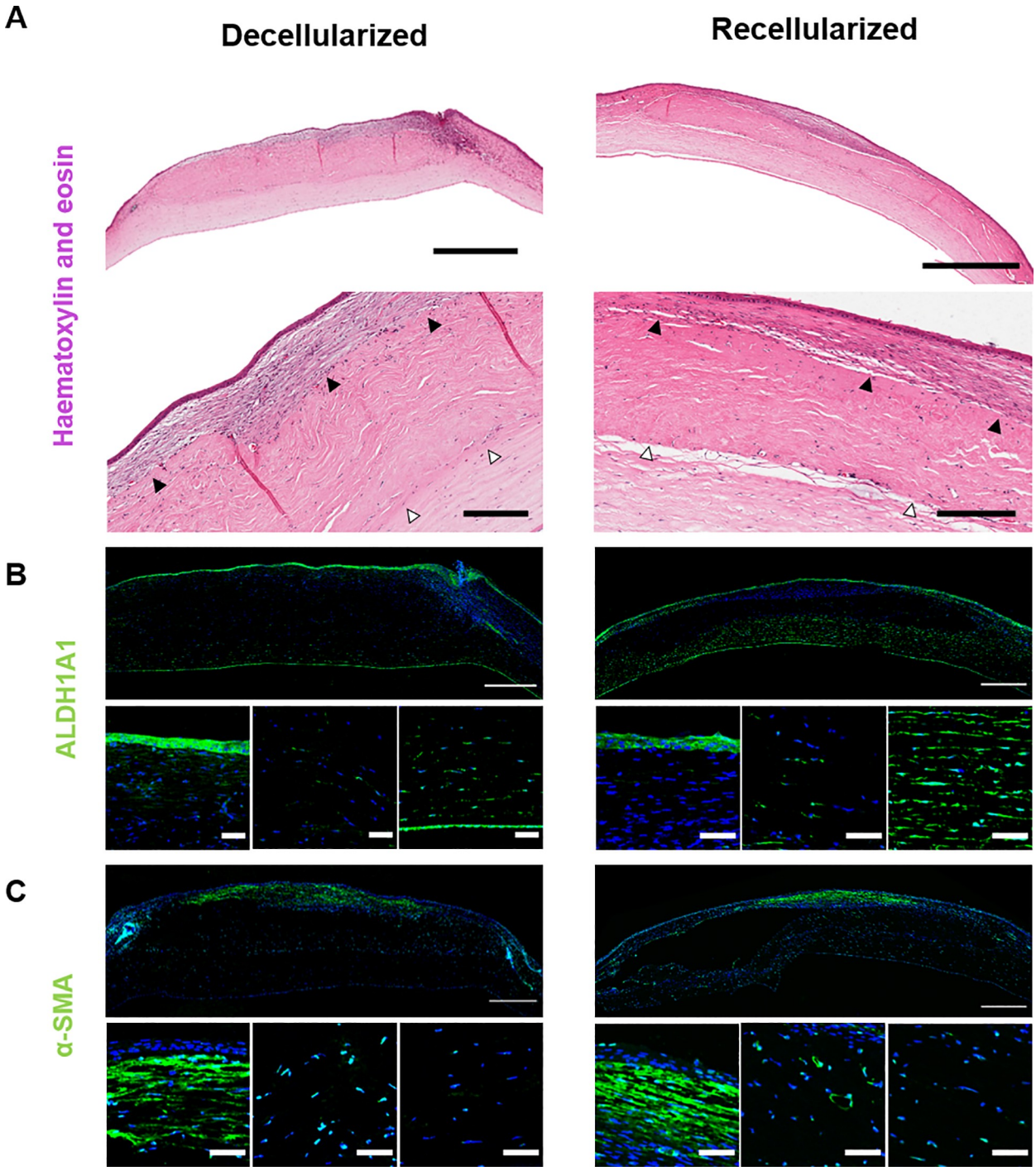

Fig 10. Rabbit cornea 3 months post-implantation stained for ECM content. Representative images comparing a decellularized scaffold (left) with a recellularized scaffold (right). Picrosirius red staining (Scale bar = 200 μm) and immunostaining against collagen I, fibronectin and collagen III, with DAPI nuclear stain (Scale bar = 500 μm). Scaffold apposed with native tissue (white arrows) and regeneration area anterior to the scaffold (black arrows). The anterior regeneration area appears denser and the fibronectin more pronounced in the recellularized implant, but the other markers are similar. The Descemet's membrane separation is a processing artefact.

https://doi.org/10.1371/journal.pone.0245406.g010

them to become more fibroblastic. To recover quiescence, i.e. an *in vivo*-like phenotype, the serum was removed from the medium in the keratocytic-expansion. This phenotype change was confirmed not only by the expression of the keratocyte cellular markers of ALDH3A1, but

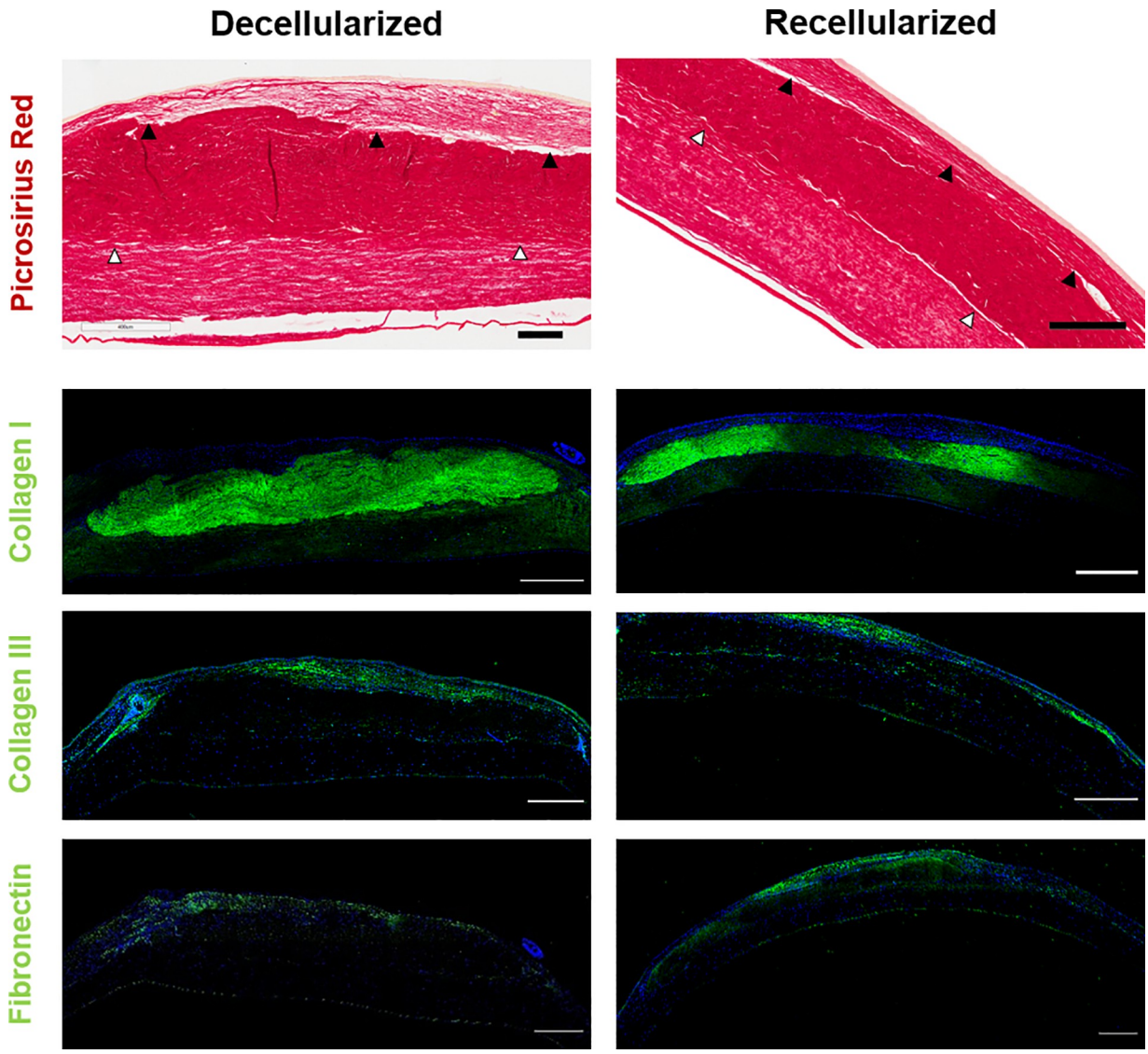

Fig 11. Rabbit cornea 3 months post-implantation stained for cell distribution and phenotype. Representative images of decellularized (left) and recellularized implant (right). A) H&E staining (Scale bar = 1 mm, 200 μm, low and high magnifications). Scaffold apposed with native tissue (white arrows) and regeneration area anterior to the scaffold (black arrows). B) Immunostaining for ALDH1A1 and, C) for α-SMA. B) and C) larger image is whole cornea with close-ups of anterior regenerating layer, central scaffold and posterior native cornea. (Scale bar = 500 μm, 50 μm, low and high magnifications).

https://doi.org/10.1371/journal.pone.0245406.g011

also CD34, and the increase of extracellular markers keratocan, decorin and lumican. The keratocan could not be demonstrated by immunohistochemistry, which may indicate individual cell variance of expression. However, PCR is a sensitive technique and despite seeing an increase in the levels of mRNA, the translation into a mature proteoglycan might not have been high enough to detect by immunohistochemistry. Under the keratocytic-expansion conditions, the appearance and phenotype of the cells resumed a native form of the uninjured cornea. Immunostaining for α-SMA did not occur in any of the groups, but there was an increase in gene expression with the long-expansion that was even larger with the keratocytic-expansion, indicating the cells were showing signs of moving to a myofibroblastic form.

Clinical outcomes in a rabbit ALK model

Decellularized porcine corneal scaffolds implanted into the human eye have shown different rates of stromal repopulation, ranging from multiple cells within 2 months [2] to little repopulation at 3 months [1]. The depth of the tissue removed and, consequentially, the amount of host stroma remaining may play a role in scaffold repopulation kinetics. These studies demonstrated that keratocyte repopulation can be slow and porcine decellularized tissue has different post-operative healing compared with fresh, cellularized, human cornea [1]. Thus, the recellularization used in the present study might be expected to improve healing. Our dissection and positioning of the scaffold maintained its orientation so that the anterior surface was also anterior in the host. Thus, the collagen fibre density according to depth should offer a similar biomechanical profile. Nonetheless, in our study with a rabbit host, stromal recellularization prior to implantation did not have much effect on the scaffold's survival or appearance *in vivo* over 3 months. Both groups appeared to show a regeneration area anterior to the scaffold. The lack of porcine collagen I, but the presence of collagen III in this area indicates new tissue, not reorganised scaffold, as the antibody we used for collagen III reacts against both human and rabbit, but the acellular scaffold had no human cells. It appears from this that the collagen III was from a rabbit cell source.

The phenotype of the cells in the scaffold differed from the cells in the regenerating tissue and the surrounding stroma. The phenotype in the scaffold varied with some cells staining positive for the keratocyte marker ALDH1A1, some for the myofibroblastic marker α-SMA and others for neither marker, potentially indicating a fibroblastic phenotype. We believe that the lack of transparency of the corneas was likely due to this fibrosis, most probably from host cells since a similar pattern of α-SMA and fibronectin was detected in both our decellularized and recellularized groups. While the cells in the recellularized scaffolds do not appear to aid in restoring transparency in this specific study, we do not know if the cells would have affected the transparency if there were no fibrosis present.

Epithelium restoration but stromal opacity

When a tissue is damaged, a fibrotic response is usually activated. While this response heals, it often fails to restore full function. However, in some instances such as with the cornea, healing can take a regenerative capacity whereby full function is restored, including transparency [17]. Corneal reaction to injury can be attributed to the type of wound. Scarring can be a pathogenic outcome from corneal surgery, and the appropriate epithelial repopulation and basement membrane regeneration can be key to minimize this [44]. It is known that stromal surface irregularities can induce stromal haze and promotion of myofibroblast transformation [45]. In addition, the degree of epithelial basement membrane integrity and the extent of epithelial cell cover is an important determinant of whether damage to the stroma is followed by fibrotic or regenerative repair [46]. The epithelial basement membrane acts as a barrier limiting the access of pro-scarring and inflammatory cytokines, such as TGF-β1 and IL-1β, from the epithelium and tears into the stroma [46]. The barrier is achieved by several ECMs, such as nidogens, perlecan or laminin, that are part of the basement membrane of the corneal epithelium and can bind TGF-β1 [47]. Decellularization detergents change the composition of the basement membrane [48], by reducing GAG and other components, thus compromising its barrier function. With tissue replacement, the loss of the epithelial basement membrane has been indicted to allow the free passage of these cytokines into the stroma, where they can activate keratocytes to become myofibroblasts which lay down the scar tissue that results in poor vision. In the present study, scaffolds were covered with epithelium, in agreement with other reports of 3 weeks to confluence [49, 50]. However, this delay in re-establishing the barrier between epithelium

and stroma appears to be long enough for the cytokines to trigger adverse change in the keratocytes. In previous studies where the defect was small (2 mm diameter) [2], there was little haze, whereas with a similar treatment but a larger defect (6 mm diameter), the haze was greater [3], as in the present study. This difference may be attributed to a lower cytokine load via the smaller diameter hole. Once the basement membrane is fully regenerated, no more activation of myofibroblasts occurs, and these undergo apoptosis and so, with time, the keratocytes may revert the scar [51]. In the animal study of Hashimoto et al. 2019 [6], the 8-week corneal appearance was similar to the current study, but at 24 months, corneal transparency was improved. From this, we might expect that if our implants had been left in place for longer, there may have been optical improvement. However, even if transparency had eventually returned, this would not have been an acceptable outcome. The study was to compare cellular with acellular corneal implants, testing for an improvement with cellular. Even if there had been a difference between groups after the 3 month experiment term, the initial disability from stromal opacification is unacceptable.

The study did not gather data on the survival kinetics of the human keratocytes, but previous studies have indicated they survive in this model for 150 days [10]. Future studies should specifically match cell origin and phenotype, as it may be the case that the human cells in our study did not survive long enough to exert sufficient benefit.

Reinnervation will be dependent upon scaffold organisation

Nerves are severed during human corneal transplantation. Following the use of human tissue allografts, some stromal nerves can appear after 2 months, but basal epithelium re-innervation might not occur until 2 years post-surgery, with corneal sensitivity being recovered no earlier than 3 years [52, 53]. In the present study rat neurites were able to extend though the full depth of the scaffold within 14 days *in vitro* and so the scaffold does not appear cytotoxic, but the environment will differ *in vivo*. In a previous study of decellularized porcine scaffold, nerves only returned in 2 out of 27 cases at 6 months and in only 3 more by 12 months [1]. Nevertheless, it would appear that the extent of reinnervation in porcine scaffold may approach that of native human allografts. Furthermore, if a collagen hydrogel is the implant, then nerve sensitivity can return much more quickly [54]. This may occur because the soft hydrogel permits reduced resistance to penetration and, if this is the case, reinstating keratocytes with a phenotype that can best restore the proteoglycan ground substance between the collagen fibrils may be of benefit.

Alternative methods to address damage from epithelial cytokines

Pocket implants, where the epithelium and its basement membrane are left in place, are not suitable for many surgeries. With ALK, damage to the epithelial basement membrane occurs during decellularized scaffold implantation and this can be detrimental to keratocyte function. Various avenues to prevent this are available which include: 1) re-epithelization *in vitro* to preoperatively restore the epithelial basement membrane to the implant, 2) prior to implantation, constituent compounds of the epithelial basement membrane, such as laminin, could be layered onto the scaffold to form a smooth barrier to movement of adverse epithelial and tear cytokines before the epithelial layer has time to restore, or 3) drug treatment might be used to counteract these cytokines, allowing keratocytes to migrate from the host, but avoiding their transformation to produce scar tissue. Of these three avenues, prior re-epithelialization with amniotic epithelial cells has been employed [55], but this reintroduces cells and the associated potential immunogenic problem. Adding laminin has also been used in experimental work with compressed collagen gels [56], hyaluronic acid hydrogels [57] and 3D bioprinted corneas

[58], but further studies are required. Drug treatment may present thee best opportunity to provide the time for the host epithelial layer to re-establish along with its basement membrane and also time to allow keratocytes to migrate from the host whilst avoiding transformation into myofibroblasts. We have previously shown that biochemical cues can be used to modulate the human corneal stromal cell phenotype to prevent myofibroblast differentiation and in some cases increase proliferation [59]. With corneal endothelium, a TGF-β inhibitor SB431542 has also been used to counteract fibroblastic phenotypes [60], and aid stromal re-innervation [61]. Such techniques of biochemical inhibition and manipulation have potential to augment the use of porcine decellularized corneal scaffold.

5. Conclusions

We successfully obtained scaffolds from decellularized porcine corneas with a low DNA and contaminate content that readily supported the growth of epithelial cells and innervation of rat nerve cells *in vitro*. The technique also allowed recellularization of keratocytes deep into the scaffold with a keratocyte-like phenotype and this may also be possible in a shorter timeframe than our 28-day culture. However, with the *in vivo* ALK rabbit model, there was little difference in the ophthalmic outcome between a decellularized and recellularized scaffold in the 3 month time frame of the study. If the study had been over a longer time-course the eventual optical outcome might have improved, but in humans, a period of corneal haze for this length of time, possible scar tissue and an extended period to clarity, is unacceptable for routine use. Our results indicate that recellularization of decellularized pig cornea with keratocytes was not sufficiently beneficial to warrant introducing stromal cells. However, this does not mean that cells should not be used in future studies, just that there was no benefit in this specific study. A different result might have been obtained using a different scaffold, seeding technique or cell concentration. Therefore, it is important when evaluating cell-seeded corneal scaffolds *in vivo*, that scaffolds without cells are used as controls to determine if the cells have any beneficial or detrimental effect. In future studies, treatment of the stromal environment may also be beneficial to limit cytokine influence on the cells.

Supporting information

S1 Fig.
(TIF)

S1 Raw image.
(PDF)

Acknowledgments

We thank the Dublin City University for animal facilities.

Author Contributions

Conceptualization: Mark Ahearne.

Data curation: Julia Fernández-Pérez, Peter W. Madden, Mark Ahearne.

Formal analysis: Julia Fernández-Pérez, Peter W. Madden.

Funding acquisition: Mark Ahearne.

Investigation: Julia Fernández-Pérez, Peter W. Madden, Robert Thomas Brady, Peter F. Nowlan.

Methodology: Julia Fernández-Pérez, Peter W. Madden, Mark Ahearne.

Project administration: Peter W. Madden, Mark Ahearne.

Resources: Mark Ahearne.

Supervision: Mark Ahearne.

Validation: Julia Fernández-Pérez.

Visualization: Julia Fernández-Pérez.

Writing – original draft: Peter W. Madden.

Writing – review & editing: Julia Fernández-Pérez, Peter W. Madden, Robert Thomas Brady, Peter F. Nowlan, Mark Ahearne.

References

1. Li S, Deng Y, Tian B, Huang H, Zhang H, Yang R, et al. Healing characteristics of acellular porcine corneal stroma following therapeutic keratoplasty. Xenotransplantation. 2019:e12566. Epub 2019/11/07. https://doi.org/10.1111/xen.12566 PMID: 31692139.
2. Shi Y, Bikkuzin T, Song Z, Jin X, Jin H, Li X, et al. Comprehensive evaluation of decellularized porcine corneal after clinical transplantation. Xenotransplantation. 2017; 24(6). Epub 2017/09/26. https://doi.org/10.1111/xen.12338 PMID: 28944512.
3. Zheng J, Huang X, Zhang Y, Wang Y, Qin Q, Lin L, et al. Short-term results of acellular porcine corneal stroma keratoplasty for herpes simplex keratitis. Xenotransplantation. 2019; 26(4):e12509. Epub 2019/04/11. https://doi.org/10.1111/xen.12509 PMID: 30968461.
4. Zhang MC, Liu X, Jin Y, Jiang DL, Wei XS, Xie HT. Lamellar keratoplasty treatment of fungal corneal ulcers with acellular porcine corneal stroma. Am J Transplant. 2015; 15(4):1068–75. https://doi.org/10.1111/ajt.13096 PMID: 25762108.
5. Alió Del Barrio JL, El Zarif M, Azaar A, Makdissy N, Khalil C, Harb W, et al. Corneal stroma enhancement with decellularized stromal laminas with or without stem cell recellularization for advanced keratoconus. Am J Ophthalmol. 2018; 186:47–58. Epub 2017/11/07. https://doi.org/10.1016/j.ajo.2017.10.026 PMID: 29103962.
6. Hashimoto Y, Funamoto S, Sasaki S, Negishi J, Hattori S, Honda T, et al. Re-epithelialization and remodeling of decellularized corneal matrix in a rabbit corneal epithelial wound model. Mater Sci Eng C Mater Biol Appl. 2019; 102:238–46. Epub 2019/05/31. https://doi.org/10.1016/j.msec.2019.04.024 PMID: 31146996.
7. Alió del Barrio JL, Chiesa M, Garagorri N, Garcia-Urquia N, Fernandez-Delgado J, Bataille L, et al. Acellular human corneal matrix sheets seeded with human adipose-derived mesenchymal stem cells integrate functionally in an experimental animal model. Exp Eye Res. 2015; 132:91–100. Epub 2015/01/28. https://doi.org/10.1016/j.exer.2015.01.020 PMID: 25625506.
8. Du L, Wu X. Development and characterization of a full-thickness acellular porcine cornea matrix for tissue engineering. Artif Organs. 2011; 35(7):691–705. Epub 2011/04/20. https://doi.org/10.1111/j.1525-1594.2010.01174.x PMID: 21501189.
9. Pang K, Du L, Wu X. A rabbit anterior cornea replacement derived from acellular porcine cornea matrix, epithelial cells and keratocytes. Biomaterials. 2010; 31(28):7257–65. Epub 2010/07/06. https://doi.org/10.1016/j.biomaterials.2010.05.066 PMID: 20598368.
10. Diao JM, Pang X, Qiu Y, Miao Y, Yu MM, Fan TJ. Construction of a human corneal stromal equivalent with non-transfected human corneal stromal cells and acellular porcine corneal stromata. Exp Eye Res. 2015; 132:216–24. Epub 2015/01/24. https://doi.org/10.1016/j.exer.2015.01.015 PMID: 25613074.
11. Fernández-Pérez J, Ahearne M. Decellularization and recellularization of cornea: Progress towards a donor alternative. Methods. 2019. Epub 2019/05/28. https://doi.org/10.1016/j.ymeth.2019.05.009 PMID: 31128238.
12. Hashimoto Y, Funamoto S, Sasaki S, Honda T, Hattori S, Nam K, et al. Preparation and characterization of decellularized cornea using high-hydrostatic pressurization for corneal tissue engineering. Biomaterials. 2010; 31(14):3941–8. https://doi.org/10.1016/j.biomaterials.2010.01.122 PMID: 20163852.
13. Maurice DM. The structure and transparency of the cornea. J Physiol. 1957; 136(2):263–86. Epub 1957/04/30. https://doi.org/10.1113/jphysiol.1957.sp005758 PMID: 13429485.

14. Goldman JN, Benedek GB. The relationship between morphology and transparency in the nonswelling corneal stroma of the shark. Invest Ophthalmol. 1967; 6(6):574–600. Epub 1967/12/01. PMID: 6073962.

15. Fini ME. Keratocyte and fibroblast phenotypes in the repairing cornea. Prog Retin Eye Res. 1999; 18 (4):529–51. Epub 1999/04/27. https://doi.org/10.1016/s1350-9462(98)00033-0 PMID: 10217482.

16. Wu J, Du Y, Mann MM, Funderburgh JL, Wagner WR. Corneal stromal stem cells versus corneal fibroblasts in generating structurally appropriate corneal stromal tissue. Exp Eye Res. 2014; 120:71–81. Epub 2014/01/21. https://doi.org/10.1016/j.exer.2014.01.005 PMID: 24440595.

17. Wilson SL, El Haj AJ, Yang Y. Control of scar tissue formation in the cornea: strategies in clinical and corneal tissue engineering. Journal of Functional Biomaterials. 2012; 3(3):642–87. https://doi.org/10.3390/jfb3030642 PMID: 24955637.

18. Yam GH, Williams GP, Setiawan M, Yusoff NZ, Lee XW, Htoon HM, et al. Nerve regeneration by human corneal stromal keratocytes and stromal fibroblasts. Sci Rep. 2017; 7:45396. Epub 2017/03/30. https://doi.org/10.1038/srep45396 PMID: 28349952.

19. Xu B, Song Z, Fan T. Construction of anterior hemi-corneal equivalents using nontransfected human corneal cells and transplantation in dog models. Artif Organs. 2017; 41(11):1004–16. Epub 2017/06/18. https://doi.org/10.1111/aor.12878 PMID: 28621916.

20. Lynch AP, Wilson SL, Ahearne M. Dextran preserves native corneal structure during decellularization. Tissue Eng Part C Methods. 2016; 22(6):561–72. Epub 2016/04/14. https://doi.org/10.1089/ten.TEC.2016.0017 PMID: 27068608.

21. Lin Y, Zheng Q, Hua S, Meng Y, Chen W, Wang Y. Cross-linked decellularized porcine corneal graft for treating fungal keratitis. Sci Rep. 2017; 7(1):9955. Epub 2017/09/01. https://doi.org/10.1038/s41598-017-08207-3 PMID: 28855517.

22. Yoeruek E, Bayyoud T, Maurus C, Hofmann J, Spitzer MS, Bartz-Schmidt KU, et al. Decellularization of porcine corneas and repopulation with human corneal cells for tissue-engineered xenografts. Acta Ophthalmol. 2012; 90(2):e125–31. https://doi.org/10.1111/j.1755-3768.2011.02261.x PMID: 22136333.

23. Lynch AP, O'Sullivan F, Ahearne M. The effect of growth factor supplementation on corneal stromal cell phenotype *in vitro* using a serum-free media. Exp Eye Res. 2016; 151:26–37. Epub 2016/07/28. https://doi.org/10.1016/j.exer.2016.07.015 PMID: 27456135.

24. West-Mays JA, Dwivedi DJ. The keratocyte: corneal stromal cell with variable repair phenotypes. Int J Biochem Cell Biol. 2006; 38(10):1625–31. Epub 2006/05/06. https://doi.org/10.1016/j.biocel.2006.03.010 PMID: 16675284.

25. Wilson SL, Wimpenny I, Ahearne M, Rauz S, El Haj AJ, Yang Y. Chemical and topographical effects on cell differentiation and matrix elasticity in a corneal stromal layer model. Adv Funct Mater. 2012; 22 (17):3641–9. https://doi.org/10.1002/adfm.201200655

26. Jester JV, Budge A, Fisher S, Huang J. Corneal keratocytes: phenotypic and species differences in abundant protein expression and in vitro light-scattering. Invest Ophthalmol Vis Sci. 2005; 46(7):2369–78. Epub 2005/06/28. https://doi.org/10.1167/iovs.04-1225 PMID: 15980224.

27. Kafienah W, Sims TJ. Biochemical methods for the analysis of tissue-engineered cartilage. Methods Mol Biol. 2004; 238:217–30. Epub 2004/02/19. https://doi.org/10.1385/1-59259-428-x:217 PMID: 14970450.

28. Ignat'eva NY, Danilov NA, Averkiev SV, Obrezkova MV, Lunin VV, Sobol' EN. Determination of hydroxyproline in tissues and the evaluation of the collagen content of the tissues. J Anal Chem. 2007; 62(1):51–7. https://doi.org/10.1134/s106193480701011x

29. Fernández-Pérez J, Madden PW, Ahearne M. Engineering a corneal stromal equivalent using a novel multi-layered fabrication assembly technique. Tissue Eng Part A. 2020; 26(19–20):1030–41. Epub 2020/05/06. https://doi.org/10.1089/ten.TEA.2020.0019 PMID: 32368948.

30. Liu W, Merrett K, Griffith M, Fagerholm P, Dravida S, Heyne B, et al. Recombinant human collagen for tissue engineered corneal substitutes. Biomaterials. 2008; 29(9):1147–58. https://doi.org/10.1016/j.biomaterials.2007.11.011 PMID: 18076983.

31. Brady RT, Madden PW. The use of animal models to assess engineered corneal tissue. In: Ahearne M, editor. Corneal Regeneration 2145. New York, NY: Humana; 2020.

32. Shafiq MA, Gemeinhart RA, Yue BYJT, Djalilian AR. Decellularized Human Cornea for Reconstructing the Corneal Epithelium and Anterior Stroma. Tissue Engineering Part C: Methods. 2012; 18:340–8. https://doi.org/10.1089/ten.tec.2011.0072 PMID: 22082039.

33. González-Andrades M, de la Cruz Cardona J, Ionescu AM, Campos A, Del Mar Perez M, Alaminos M. Generation of bioengineered corneas with decellularized xenografts and human keratocytes. Invest

Ophthalmol Vis Sci. 2011; 52(1):215–22. Epub 2010/08/27. https://doi.org/10.1167/iovs.09-4773 PMID: 20739475.

34. Fernández-Pérez J, Binner M, Werner C, Bray LJ. Limbal stromal cells derived from porcine tissue demonstrate mesenchymal characteristics *in vitro*. Sci Rep. 2017; 7(1):6377. Epub 2017/07/27. https://doi.org/10.1038/s41598-017-06898-2 PMID: 28743889.

35. Guyette JP, Gilpin SE, Charest JM, Tapias LF, Ren X, Ott HC. Perfusion decellularization of whole organs. Nat Protoc. 2014; 9:1451–68. https://doi.org/10.1038/nprot.2014.097 PMID: 24874812.

36. Alhamdani MSS, Schröder C, Werner J, Giese N, Bauer A, Hoheisel JD. Single-step procedure for the isolation of proteins at near-native conditions from mammalian tissue for proteomic analysis on antibody microarrays. J Proteome Res. 2010; 9(2):963–71. https://doi.org/10.1021/pr900844q PMID: 20047340

37. Sasaki S, Funamoto S, Hashimoto Y, Kimura T, Honda T, Hattori S, et al. *In vivo* evaluation of a novel scaffold for artificial corneas prepared by using ultrahigh hydrostatic pressure to decellularize porcine corneas. Mol Vis. 2009; 15:2022–8. Epub 2009/10/22. PMID: 19844587.

38. Crapo PM, Gilbert TW, Badylak SF. An overview of tissue and whole organ decellularization processes. Biomaterials. 2011; 32:3233–43. https://doi.org/10.1016/j.biomaterials.2011.01.057 PMID: 21296410.

39. Zheng MH, Chen J, Kirilak Y, Willers C, Xu J, Wood D. Porcine small intestine submucosa (SIS) is not an acellular collagenous matrix and contains porcine DNA: possible implications in human implantation. J Biomed Mater Res B Appl Biomater. 2005; 73(1):61–7. Epub 2005/03/01. https://doi.org/10.1002/jbm.b.30170 PMID: 15736287.

40. Macher BA, Galili U. The Galα1,3Galβ1,4GlcNAc-R (α-Gal) epitope: a carbohydrate of unique evolution and clinical relevance. Biochim Biophys Acta. 2008; 1780(2):75–88. Epub 2007/12/01. https://doi.org/10.1016/j.bbagen.2007.11.003 PMID: 18047841.

41. Lee W, Miyagawa Y, Long C, Cooper DK, Hara H. A comparison of three methods of decellularization of pig corneas to reduce immunogenicity. Int J Ophthalmol. 2014; 7(4):587–93. https://doi.org/10.3980/j.issn.2222-3959.2014.04.01 PMID: 25161926.

42. Kim MK, Hara H. Current status of corneal xenotransplantation. Int J Surg. 2015; 23(Pt B):255–60. Epub 2015/08/02. https://doi.org/10.1016/j.ijsu.2015.07.685 PMID: 26231995.

43. Friedrich EE, Lanier ST, Niknam-Bienia S, Arenas GA, Rajendran D, Wertheim JA, et al. Residual sodium dodecyl sulfate in decellularized muscle matrices leads to fibroblast activation *in vitro* and foreign body response *in vivo*. J Tissue Eng Regen Med. 2018; 12(3):e1704–e15. Epub 2017/10/31. https://doi.org/10.1002/term.2604 PMID: 29084373.

44. Torricelli AAM, Santhanam A, Wu J, Singh V, Wilson SE. The corneal fibrosis response to epithelial–stromal injury. Exp Eye Res. 2016; 142:110–8. https://doi.org/10.1016/j.exer.2014.09.012 PMID: 26675407.

45. Netto MV, Mohan RR, Sinha S, Sharma A, Dupps W, Wilson SE. Stromal haze, myofibroblasts, and surface irregularity after PRK. Exp Eye Res. 2006; 82(5):788–97. https://doi.org/10.1016/j.exer.2005.09.021 PMID: 16303127.

46. Stramer BM, Zieske JD, Jung JC, Austin JS, Fini ME. Molecular mechanisms controlling the fibrotic repair phenotype in cornea: implications for surgical outcomes. Invest Ophthalmol Vis Sci. 2003; 44(10):4237–46. Epub 2003/09/26. https://doi.org/10.1167/iovs.02-1188 PMID: 14507867.

47. Medeiros CS, Marino GK, Santhiago MR, Wilson SE. The corneal basement membranes and stromal fibrosis. Invest Ophthalmol Vis Sci. 2018; 59(10):4044–53. Epub 2018/08/12. https://doi.org/10.1167/iovs.18-24428 PMID: 30098200.

48. Faulk DM, Carruthers CA, Warner HJ, Kramer CR, Reing JE, Zhang L, et al. The effect of detergents on the basement membrane complex of a biologic scaffold material. Acta Biomater. 2014; 10(1):183–93. Epub 2013/09/24. https://doi.org/10.1016/j.actbio.2013.09.006 PMID: 24055455.

49. Hashimoto Y, Funamoto S, Sasaki S, Negishi J, Honda T, Hattori S, et al. Corneal regeneration by deep anterior lamellar keratoplasty (DALK) using decellularized corneal matrix. PLoS ONE. 2015; 10(7):e0131989. Epub 2015/07/15. https://doi.org/10.1371/journal.pone.0131989 PMID: 26161854.

50. Huang Y-H, Tseng F-W, Chang W-H, Peng IC, Hsieh D-J, Wu S-W, et al. Preparation of acellular scaffold for corneal tissue engineering by supercritical carbon dioxide extraction technology. Acta Biomater. 2017; 58:238–43. https://doi.org/10.1016/j.actbio.2017.05.060 PMID: 28579539.

51. Mohan RR, Hutcheon AEK, Choi R, Hong J, Lee J, Mohan RR, et al. Apoptosis, necrosis, proliferation, and myofibroblast generation in the stroma following LASIK and PRK. Exp Eye Res. 2003; 76(1):71–87. https://doi.org/10.1016/s0014-4835(02)00251-8 PMID: 12589777.

52. Darwish T, Brahma A, Efron N, O'Donnell C. Subbasal nerve regeneration after penetrating keratoplasty. Cornea. 2007; 26(8):935–40. Epub 2007/08/28. https://doi.org/10.1097/ICO.0b013e3180de493f PMID: 17721291.

53. Richter A, Slowik C, Somodi S, Vick HP, Guthoff R. Corneal reinnervation following penetrating keratoplasty-correlation of esthesiometry and confocal microscopy. Ger J Ophthalmol. 1996; 5(6):513–7. Epub 1996/11/01. PMID: 9479548.

54. Islam MM, Buznyk O, Reddy JC, Pasyechnikova N, Alarcon EI, Hayes S, et al. Biomaterials-enabled cornea regeneration in patients at high risk for rejection of donor tissue transplantation. NPJ Regen Med. 2018; 3:2. Epub 2018/02/10. https://doi.org/10.1038/s41536-017-0038-8 PMID: 29423280.

55. Luo H, Lu Y, Wu T, Zhang M, Zhang Y, Jin Y. Construction of tissue-engineered cornea composed of amniotic epithelial cells and acellular porcine cornea for treating corneal alkali burn. Biomaterials. 2013; 34(28):6748–59. Epub 2013/06/15. https://doi.org/10.1016/j.biomaterials.2013.05.045 PMID: 23764112.

56. Gouveia RM, Lepert G, Gupta S, Mohan RR, Paterson C, Connon CJ. Assessment of corneal substrate biomechanics and its effect on epithelial stem cell maintenance and differentiation. Nat Commun. 2019; 10(1):1496. Epub 2019/04/05. https://doi.org/10.1038/s41467-019-09331-6 PMID: 30944320.

57. Koivusalo L, Kauppila M, Samanta S, Parihar VS, Ilmarinen T, Miettinen S, et al. Tissue adhesive hyaluronic acid hydrogels for sutureless stem cell delivery and regeneration of corneal epithelium and stroma. Biomaterials. 2019; 225:119516. Epub 2019/10/02. https://doi.org/10.1016/j.biomaterials.2019.119516 PMID: 31574405.

58. Sorkio A, Koch L, Koivusalo L, Deiwick A, Miettinen S, Chichkov B, et al. Human stem cell based corneal tissue mimicking structures using laser-assisted 3D bioprinting and functional bioinks. Biomaterials. 2018; 171:57–71. Epub 2018/04/24. https://doi.org/10.1016/j.biomaterials.2018.04.034 PMID: 29684677.

59. Fernández-Pérez J, Ahearne M. Influence of biochemical cues in human corneal stromal cell phenotype. Curr Eye Res. 2019; 44(2):135–46. Epub 2018/10/20. https://doi.org/10.1080/02713683.2018.1536216 PMID: 30335528.

60. Okumura N, Kay EP, Nakahara M, Hamuro J, Kinoshita S, Koizumi N. Inhibition of TGF-β signaling enables human corneal endothelial cell expansion *in vitro* for use in regenerative medicine. PLoS ONE. 2013; 8(2):e58000. Epub 2013/03/02. https://doi.org/10.1371/journal.pone.0058000 PMID: 23451286.

61. Jeon KI, Hindman HB, Bubel T, McDaniel T, DeMagistris M, Callan C, et al. Corneal myofibroblasts inhibit regenerating nerves during wound healing. Sci Rep. 2018; 8(1):12945. Epub 2018/08/30. https://doi.org/10.1038/s41598-018-30964-y PMID: 30154512.